
Towards Revealing the Effectiveness of Small-Scale Fine-tuning in R1-style Reinforcement Learning

Yutong Chen*
 Tsinghua University
 Beijing, China
 chen-yt23@mails.tsinghua.edu.cn

Jiandong Gao[†]
 Tsinghua University
 Beijing, China
 jdgao@tsinghua.edu.cn

Ji Wu[‡]
 Tsinghua University
 Beijing, China
 wuji_ee@tsinghua.edu.cn

Abstract

R1-style Reinforcement Learning (RL) significantly enhances Large Language Models' reasoning capabilities, yet the mechanism behind rule-based RL remains unclear. We found that small-scale SFT has significant influence on RL but shows poor efficiency. To explain our observations, we propose an analytical framework and compare the efficiency of SFT and RL by measuring **sample effect**. Hypothetical analysis show that SFT efficiency is limited by training data. Guided by our analysis, we propose **Re-distillation**, a technique that fine-tunes pretrain model through small-scale distillation from the RL-trained policy. Experiments on Knight & Knave and MATH datasets demonstrate re-distillation's surprising efficiency: re-distilled models match RL performance with far fewer samples and less computation. Empirical verification shows that sample effect is a good indicator of performance improvements. As a result, on K&K dataset, our re-distilled Qwen2.5-1.5B model surpasses DeepSeek-V3-0324 with only 1K SFT samples. On MATH, Qwen2.5-1.5B fine-tuned with re-distilled 500 samples matches its instruct-tuned variant without RL. Our work explains several interesting phenomena in R1-style RL, shedding light on the mechanisms behind its empirical success. Code is available at: <https://github.com/on1262/deep-reasoning>

1 Introduction

Recent advances in Reinforcement Learning for Large Language Models (LLMs) demonstrate remarkable improvements in reasoning-intensive tasks (Guo et al., 2025; Kimi Team et al., 2025; Qwen Team, 2025; OpenAI et al., 2024, 2025). We define R1-style RL as outcome-based reinforcement learning that evaluates final correctness without step-wise verification. This approach typically involves two phases: Supervised Fine-Tuning (SFT), where models learn instruction-following and long Chain-of-Thought (Wei et al., 2022) through curated reasoning sequences, followed by RL optimization. Empirical evidence suggests improving SFT quality enhances subsequent RL performance. For instance, DeepSeek-R1 employed carefully filtered reasoning traces from DeepSeek-R1-Zero

*M.S. student. Department of Electronic Engineering

[†]Ph.D. Corresponding author. Department of Electronic Engineering

[‡]Ph.D. Corresponding author. Department of Electronic Engineering; College of AI, Tsinghua University; Beijing National Research Center for Information Science and Technology, Beijing, China

(Guo et al., 2025). In this paper, we focus on **small-scale SFT** ($\leq 2K$ samples or 50M tokens), enabling manual sample inspection while ensuring performance gains mainly from reasoning capability elicitation rather than knowledge expansion.

The relationship between SFT and RL seems like a paradox: while SFT provides richer supervision, RL remains essential for further improvement (Chu et al., 2025). Recent works found strong memorization effect during LLM pretraining, recalling rare information from minimal exposure (Hartmann et al., 2023; Carlini et al., 2022). On the contrary, rule-based RL is under severe information constraints. A binary reward function with solution correctness probability p conveys merely $H = -p\log p - (1-p)\log(1-p) \leq 1$ bit on average.

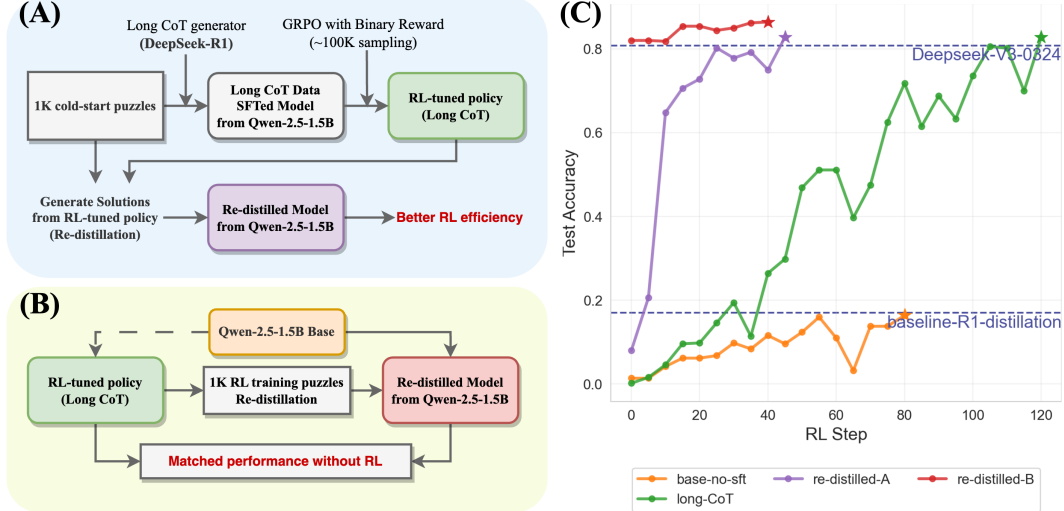


Fig. 1. Main experiments overview. **Left (A):** On K&K dataset, we distill 1K long Chain-of-Thought data from DeepSeek-R1 to train SFTed model. After GRPO, long CoT initialized policy(long-CoT) shows remarkable improvement compared with other models. Then we re-distill RL-trained policy with the same 1K puzzles. The re-distilled policy(re-distilled-A), trained from Qwen2.5-1.5B base, reveals much faster convergence in RL. **Left (B):** We randomly pick 1K puzzles from RL training set and generate solutions from RL-trained policy, then re-distill Qwen2.5-1.5B to train re-distilled-B. As a result, re-distilled-B matched long-CoT immediately after finetuning, revealing the possibility to reproduce RL-trained policy's performance without RL. The baseline(baseline-R1-distillation, horizontal line in Right(C)) is distilled from DeepSeek-R1 with the same question but performs significantly worse. **Right (C):** We run GRPO for two re-distilled models, long-CoT initialized policy and base model(base-no-sft). Re-distillation is able to ‘compress’ RL’s progress with only SFT. Experiments on MATH dataset are similar. See section 4 for further details.

Our study starts from examining SFT efficiency through experiments on K&K (Xie et al., 2024) and MATH (Hendrycks et al., 2021), a specific and a general reasoning dataset. An overview is depicted in Figure 1. Firstly, we wonder if small-scale fine-tuning has significant effect. We construct SFT datasets using DeepSeek-R1 distilled long CoT data⁴. Fine-tuning Qwen2.5-1.5B Base model with $\approx 1K$ samples reveals that small-scale SFT brings significant influence on RL stage. We explain our observations by establishing an analytic framework. Under the hypothesis that non-linear training dynamic of RL can be analyzed by linearized model, the effectiveness of both RL and SFT can be decomposed to each sample’s contribution. We name this contribution as **sample effect**. We prove that sample effect has great influence on SFT effectiveness. Specifically, the optimal policy for distillation outputs samples with high effect. We also proved that RL improves output sample effect and test performance simultaneously, which suggests the potential of learning from RL-trained policy.

⁴In this paper, both distillation and re-distillation use hard labels (token IDs). We do not fit token distribution by soft label.

Inspired by hypothetical analysis, we propose the **Re-distillation** technique to discover the full potential of small-scale SFT. This method samples from converged policy to generate new SFT data. Remarkably, base models trained on re-distilled data match converged RL performance using only SFT, demonstrating superior data efficiency. Empirical verification shows high alignment between sample effect and experimental training results.

This work provides novel insights into small-scale SFT’s efficiency and establishes a method to measure RL-induced improvement in both theoretical and empirical ways. Unlike prior studies (Ye et al., 2025; Chu et al., 2025; Gandhi et al., 2025), we emphasize the *model-specific SFT effectiveness*, demonstrating that data quality is not the dominant factor. Additionally, the effectiveness of re-distillation is non-trivial. It can not be reproduced by more SFT data or higher randomness in exploration (Appendix C).

Our main contributions and findings are listed as follows:

- We demonstrate that SFT can be as generalizable as RL. Fewer than 1K SFT samples reproduces RL’s performance. We propose Re-distillation as a *post-hoc* method for creating high-efficiency SFT datasets (section 6).
- Our hypothetical analysis reveals that the poor sample efficiency is not an intrinsic property of SFT. SFT training dynamic is influenced by *sample effects* (subsection 5.2). We provide empirical study to verify our hypothesis (subsection 6.1).
- We explain why re-distillation is so effective. Specifically, we proved a lower bound of output sample effect on RL-trained policy which relate to the reward growth rate (subsection 5.3).
- We explain why SFT influence RL exploration in the long term. Our experiment shows RL’s inherent difficulty in modifying initial token distributions compared to SFT subsection 6.2.

2 Related Works

SFT in R1-style Reinforcement Learning: Recent studies demonstrate small-scale SFT’s significant impact on subsequent RL performance. Gandhi et al. (2025) shows Qwen2.5-3B (Yang et al., 2024b) and Llama3-3B (Grattafiori et al., 2024) benefit from 1K SFT samples in reasoning tasks. Yeo et al. (2025) finds high-quality SFT data is crucial for releasing RL potential. Notably, Zeng et al. (2025) reports degraded performance with short CoT data than RL on base models, though direct RL on base models risks poor instruction following Chu et al. (2025). Xie et al. (2025) finds nearly identical reward curves when applying RL to both base and instruction-tuned Qwen2.5-7B models. Zhao et al. (2025) observes RL tends to fall into single pretrain mode. Common observations include unstable response length growth and the pre-existence of reasoning patterns in base models (Zeng et al., 2025; Xie et al., 2025; Yeo et al., 2025).

Direct SFT Approaches: Emerging research achieves remarkable results through small-scale SFT. By leveraging high quality data, LIMO Ye et al. (2025) elicits Qwen2.5-32B-Instruct’s reasoning capabilities and matched Qwen-QwQ-32B-Preview’s performance. Similarly, Muennighoff et al. (2025) obtains strong results with 1K SFT samples. (Carlsson et al., 2024) proposed Hyperfitting, a method to reduce repetition rate and improve output quality by overfitting small datasets. However, Li et al. (2025) finds small-scale SFT less effective than RL for smaller models like Qwen-Math-7B, suggesting scale-dependent efficiency. Chu et al. (2025) found SFT tend to memorize but not generalizable to out-of-distribution samples.

Theoretical analysis of LLM with RL: Analyzing LLM is challenging while traditional method failed to predict large neural network’s strong generalization ability (Azar et al., 2024). Ren and Sutherland (2024) established a hypothetical framework using the step-wise decomposition to explain the hallucination in SFT and the squeezing effect appeared in DPO. Neural Tangent Kernel(NTK) focus on linearized effect and achieved remarkable success in predicting the behavior of infinite wide networks (Jacot et al., 2018; Arora et al., 2019). In LLM alignment, Direct Preference Optimization(DPO) propose a practical method to bypass expensive Reinforcement Learning (Rafailov et al., 2023). Massive works based on DPO reveals both empirical and theoretical achievements (Ji et al., 2024; Ethayarajh et al., 2024).

3 Preliminaries

GRPO: We leverage GRPO for Reinforcement Learning. Although other RL algorithms have shown remarkable performance, such as DAPO (Yu et al., 2025) and REINFORCE++ (Hu, 2025), we choose GRPO because of its simplicity. GRPO aims to maximize the objective $\mathcal{J}_{GRPO}(\theta) = \mathbb{E}_{a \sim \pi_{old}(s), s \sim \mathcal{D}_{train}} [\frac{1}{G} \sum_{i=1}^G (rA_i, \text{clip}(r, 1 - \epsilon, 1 + \epsilon)A_i) - \beta \mathbb{D}_{KL}(\pi_\theta || \pi_{ref})]$, where $r(\pi_\theta, \pi_{\theta_{old}}, s, a) = \frac{\pi_\theta(s, a)}{\pi_{\theta_{old}}(s, a)}$ is the probability ratio, \mathbb{D}_{KL} is the estimated KL divergence, s represents prompt as state, a represents response as action, π_{old} denotes sampling policy, π_{ref} denotes reference(or initial) policy for KL divergence control.

Knight & Knave dataset(K&K): Knight & Knave is a logic puzzle that requires identify each person as knight or knave (Xie et al., 2024). A knight always tell the truth and a knave always lie. A puzzle contains N people with one statement for each person. K&K dataset has flexible difficulties and a large enough problem space. By increasing the number of person N_{ppl} in one puzzle, it is able to create challenging puzzle for LLM. Solving this puzzle heavily rely on verifying, back-tracking and self-correction abilities. A step-by-step solution can be synthesized automatically. We choose K&K dataset as a representative downstream task because: 1. Reasoning in K&K puzzle does not require extra domain knowledge, giving small LLMs potential to improve their ability. 2. General reasoning task often need long rollout sequences and extensive computation to observe non-trivial improvement.

4 Investigating the effectiveness of SFT

We start from investigate the effectiveness of small-scale SFT on K&K and MATH dataset. Intuitively, more thinking tokens may bring better RL convergence. Hence, we leverage DeepSeek-R1 to generate reliable long reasoning traces. We keep other settings unchanged to observe the standalone effectiveness of data.

4.1 Data Preparation

On K&K dataset, we generate 1,000 synthetic questions and solutions to build short-CoT-kk dataset with $N_{ppl} \in \{2, 3\}$. The term N_{ppl} is related to the puzzle difficulty. These samples are randomly split into 900/100 for training/validation. To obtain longer reasoning chains, we prompt DeepSeek-R1 with the same 1K questions, filtering responses exceeding 4,096 tokens or containing incorrect answers. This yields 846 samples (763 training, 83 validation) for the long-CoT-kk dataset. For reinforcement learning, we generate 2,000 samples per $N_{ppl} \in \{3, 4, 5, 6, 7\}$ for training, resulting 10K samples. The test set contains 500 samples (100 per $N_{ppl} \in \{4, 5, 6, 7, 8\}$). To evaluate out-of-distribution generalization, $N_{ppl} = 8$ samples are excluded from training set.

On MATH dataset, we leave MATH-500 test problems out and further split the rest 12K samples into 11K/900/100 for RL training, SFT training and SFT validation. The short-CoT-math dataset uses step-by-step solutions from the original dataset (Hendrycks et al., 2021). long-CoT-math contains 690 training and 75 validation samples generated similarly to long-CoT-kk. In following sections, we use -math and -kk to refer models trained on MATH/K&K dataset.

4.2 Supervised Fine-tuning and Reinforcement Learning

We fine-tune the Qwen2.5-1.5B (Yang et al., 2024a) base model for 2 epochs on both short and long CoT datasets. As a result, **small-scale SFT does not instantly improve performance**. In Figure 2, although distilled long-CoT models develop advanced reasoning behaviors (e.g., "Wait" or "Let me check"), SFT alone shows limited immediate accuracy improvements. SFT performance(step 0 accuracy) even get worse compared with base model. For example, model fine-tuned on long-CoT-math achieves 18.4% accuracy on MATH-500, which is lower than base model(23.8%).

After SFT, we collect four initial policies to perform R1-style Reinforcement Learning: `base-no-sft` (Qwen2.5-1.5B base), `instruct-no-sft` (Qwen2.5-1.5B instruct), `short-CoT` (fine-tuned on short reasoning chains), and `long-CoT` (fine-tuned on DeepSeek-R1 distilled data).

In Reinforcement Learning, we adopt a binary reward function only output 0 or 1. Positive reward is assigned only when the response is correct and within the length constraint. Additional implementation details are provided in Appendix D.

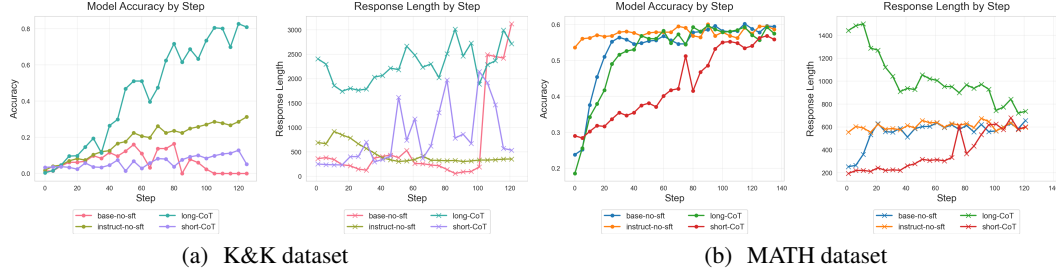


Fig. 2. Initial policy’s impact on RL convergence. Small-scale SFT has great impact but lacks of clear order or pattern. On K&K, long-CoT-kk demonstrates superior performance to the other models while maintaining longer responses. On MATH, long-CoT is slightly slower than base model and short-CoT-math shows the worst reward curve.

Our RL results (Figure 2) show several key findings. Firstly, we found that **small-scale SFT has a significant impact on RL stage but the pattern is unclear**. On K&K, long-CoT-kk achieves over 80% accuracy while maintaining responses exceeding 2,000 tokens. The training efficiency of long-CoT-kk even surpassed instruct model(instruct-no-sft-kk) with a large margin. short-CoT-math converged much slower than long CoT. However, long-CoT-kk fails to exceed 1base-no-sft on MATH dataset. Secondly, we observed **a performance ceiling in RL performance** on MATH, where all models converge to near 60% accuracy and 700-token responses, aligning with instruct model’s characteristics. Notably, **SFT performance is unreliable for predicting final RL results**. long-CoT-math shows lower initial accuracy but converges faster than short-CoT-math, and all K&K policies begin below 5% accuracy despite divergent final performance.

5 Hypothetical Analysis

5.1 Estimate Reward Growth Rate

Given significant influence of small-scale SFT, we try to explain these phenomena from a theoretical perspective. Intuitively, we need to describe “how fast test accuracy increases in training”. Let a denotes a response(action) and s denotes a prompt(state). With an evaluation dataset D_e and a policy $\pi_\theta(a, s)$, the test accuracy can be defined as $\Psi(\theta) = \mathbb{E}_{a \sim \pi_\theta, s \sim D_e} [r(a, s)]$, where $r(a, s) \in \{0, 1\}$ is a binary reward. Consider optimizing $r(a, s)$ by a basic REINFORCE (Sutton et al., 1999) algorithm and Stochastic Gradient Descent(SGD), policy gradient is computed by aggregating samples as Equation 1, where N is train batch size and D_t is training set.

$$-\nabla_\theta L = \frac{1}{N} \sum_{a \sim \pi_\theta, s \sim D_t} [\vec{\nabla}_\theta \ln \pi_\theta(a, s) r(a, s)] \quad (1)$$

When learning rate η is sufficiently small, we can describe the dynamic system by Stochastic Differential Equation(SDE): $d\vec{\theta} = -\vec{\nabla}_\theta L dt$. Since test accuracy $\Psi(\theta(t))$ is a random variable related to $\vec{\theta}$, it has mean(drift term $\mu(t, X)$) and variance(noise term, $\sigma(t, X)$) evolving with time t . We focus on the drift term $\mu(t, \Psi(\theta))$ because it measures the mean growth rate of test accuracy. We derive the growth rate of test accuracy in Equation 2. See subsection A.1 for full proof and assumptions.

$$\begin{aligned}
\mu(t, \Psi(\theta)) &= \underbrace{\mathbb{E}_{s \sim D_e, a \sim \pi_\theta} [\vec{\nabla}_\theta \ln \pi_\theta(a, s) r(a, s)]^\top \mathbb{E}_{s \sim D_t, a \sim \pi_\theta} [\vec{\nabla}_\theta \ln \pi_\theta(a, s) r(a, s)]}_{\text{Positive effect from reward signal}} \\
&\quad + \underbrace{\frac{1}{2} \frac{\eta}{N} \sum_{i=1}^n \vec{A}_i^\top \nabla^2 \Psi(\theta) \vec{A}_i}_{\text{Negative effect from noise}}
\end{aligned} \tag{2}$$

The drift term $\mu(t, \Psi(\theta))$ contains two terms. The first term is the inner product of policy gradient on training set and test set, which is non-negative when two sets are identical. It contains the positive effect from reward signal. The second term comes from gradient noise. It reveals how performance deteriorates by random disturbance. Noises also introduce instability described by $\sigma(t, X)$. However, it is challenging to compute the negative effect since it contains second order derivative $\nabla_\theta^2 \Psi$.

With large enough learning rate and train batch size, the coefficient η/N can be small, we assume that when initial policy is far from converged and suitable hyperparameter, the positive effect dominates training dynamic as initial steps. Therefore, we only compute the first term $\hat{\mu}(t, X)$ as an approximation of $\mu(t, X)$ in the following analysis.

Definition 5.1. *Given evaluation set D_e and model parameter θ , we define **sample effect** $V(a, s, \theta)$ for each prompt s and response a pair as:*

$$V(a, s, \theta) = \mathbb{E}_{s \sim D_e, a \sim \pi_\theta} [\vec{\nabla}_\theta \ln \pi_\theta(a, s) r(a, s)]^\top \vec{\nabla}_\theta \ln \pi_\theta(a, s)$$

We define the **sample effect** ($V(a, s, \theta)$) in Definition 5.1. Intuitively, it describes the contribution of a sample's gradient computed by cross-entropy loss. By introducing sample effect, the approximated growth rate $\hat{\mu}(t, X)$ can be written as a weighted average of sample effect in Equation 3.

$$\hat{\mu}_{\text{RL}}(t, \Psi(\theta)) = \mathbb{E}_{s \sim D_t, a \sim \pi_\theta} [V(a, s, \theta) r(a, s)] \tag{3}$$

5.2 Optimal Policy for Filtered Distillation

Consider generate samples from a target policy $\pi_\theta^\dagger(a, s)$ on training set and distill $\pi_\theta(a, s)$ with only correct samples. This can be viewed as distilling from $\hat{\pi}_\theta^\dagger(a, s) = \frac{\pi_\theta^\dagger(a, s)}{p_\theta^\dagger(s)} r(a, s)$ where $p_\theta^\dagger(s) = \mathbb{E}_{s \sim D_t, a \sim \pi_\theta^\dagger} [r(a, s)]$ is the accuracy for each problem s .

$$\hat{\mu}_{\text{SFT}}(t, \Psi(\theta)) = \mathbb{E}_{s \sim D_t, a \sim \hat{\pi}_\theta^\dagger} [V(a, s, \theta) r(a, s)] \tag{4}$$

Using sample effect, we compute the growth rate of SFT in Equation 4. Similarly, we can subtract them to derive how fast SFT improves than RL (Equation 5).

$$\Delta \hat{\mu}(t, \Psi(\theta)) = \hat{\mu}_{\text{SFT}}(t, \Psi(\theta)) - \hat{\mu}_{\text{RL}}(t, \Psi(\theta)) \tag{5}$$

$$= \mathbb{E}_{s \sim D_t, a \sim \pi_\theta} [V(a, s, \theta) \left(\frac{\pi_\theta^\dagger(a, s)}{p_\theta^\dagger(s) \pi_\theta(a, s)} - 1 \right) r(a, s)] \tag{6}$$

Given an initial policy π_θ and a dataset, an optimal target policy π_θ^* maximizes delta speed $\Delta \hat{\mu}(t, \Psi(\theta))$, where $p_\theta^*(s) = \mathbb{E}_{a \sim \pi_\theta^*} [r(a, s) | s]$ is a constraint on π_θ . We wonder the relationship between optimal policy and sample effect, as well as $p_\theta^*(s)$. Therefore, we compute the optimal distribution when maximizing $\Delta \hat{\mu}(t, \Psi(\theta))$ with a KL divergence constraint. The full proof of Theorem 5.1 and Corollary 5.1 is in subsection A.2.

Theorem 5.1. *Let π_θ^* to be the optimal policy for maximizing $\mathbb{E}_{s \sim D_t, a \sim \pi_\theta} [V(a, s, \theta) \left(\frac{\pi_\theta^*(a, s)}{p_\theta^*(s) \pi_\theta(a, s)} - 1 \right) r(a, s)] - \beta \mathbb{D}_{KL}[\pi_\theta^* || \pi_\theta]$ with $\beta > 0$ and $\mathbb{E}_{a \sim \pi_\theta^*} [r(a, s) | s] = p_\theta^*(s) \in (0, 1]$. For any a_1, a_2 and $s \in \{D_t\}$ that satisfies $r(a_1, s) = r(a_2, s) = 1$, we have: $\ln \frac{\pi_\theta^*(a_1, s)}{\pi_\theta^*(a_2, s)} = \frac{1}{\beta p_\theta^*(s)} (V(a_1, s, \theta) - V(a_2, s, \theta)) + \ln \frac{\pi_\theta(a_1, s)}{\pi_\theta(a_2, s)}$*

Corollary 5.1. For any optimal policy π_θ^* with $p_\theta^*(s) \in (0, 1]$ and $\beta > 0$, we can always find another β' and $p'_\theta(s)$ which satisfies $\beta p_\theta^*(s) = \beta' p'_\theta(s)$ to make the filtered optimal policy $\hat{\pi}_\theta^*$ unchanged.

In Theorem 5.1, we proved that answers with higher $V(a, s, \theta)$ tend to gain more probability mass in optimal target policy. When $V(a_1, s, \theta) > V(a_2, s, \theta)$ and β is small enough, the output probability of a_1 will be greater than a_2 . Therefore, samples with higher effect will obtain more probability mass. But does the test accuracy matter? After filtering, any target policy will only produce correct response. In Corollary 5.1, we proved that simply adjusting accuracy is identical to choosing a different β , which does not improve SFT effectiveness.

5.3 Reinforcement Learning Improves Output Sample Effect

Theorem 5.1 suggests that distillation benefits from a target policy with high output effects. Motivated by the similarity of initial policy and RL-trained policy, we investigate if RL-trained policy is more suitable. In Definition 5.2, we introduce **dataset effect**, which is a weighted average of sample effect in training set D_t . Note that we sample from filtered policy $\hat{\pi}_\theta^\dagger$ but not the original policy π_θ^\dagger .

Definition 5.2. Let π_θ^\dagger to be any policy and $\hat{\pi}_\theta^\dagger$ to be the filtered target policy. Given a training set D_t , we define the **dataset effect** as: $V(\theta, \theta^\dagger, D_t) = \mathbb{E}_{s \sim D_t, a \sim \hat{\pi}_\theta^\dagger} [V(a, s, \theta)r(a, s)]$.

Theorem 5.2. Let D_t denotes the training set and D_e denotes the evaluation set. $\hat{\mu}(t, V(\theta, \theta^*, D_t))$ denotes the approximated growth rate of dataset effect in RL. $\hat{\mu}(t, \Psi(\theta))$ denotes the approximated growth rate of reward. When $D_t = D_e$ and $\theta^* = \theta$, we have $\hat{\mu}(t, V(\theta, \theta^*, D_t)) \geq \hat{\mu}^2(t, \Psi(\theta))$.

In Theorem 5.2, we assume that RL is applied on π_θ . If we observed a positive growth rate of training accuracy $\hat{\mu}(t, \Psi(\theta))$, a positive increment of filtered dataset effect $V(\theta, \theta^*, D_t)$ is guaranteed at least in initial steps. This analysis reveals great potential of distillation from RL-trained policy. Notably, the increment is not simply come from correctness filtering because $\hat{\mu}(t, V(\theta, \theta^*, D_t)) > 0$ indicates the growth rate based on $\mathbb{E}_{s \sim D_t, a \sim \hat{\pi}_\theta^\dagger} [V(a, s, \theta)r(a, s)]$, which is already filtered.

6 Re-distillation from RL-trained Models

Inspired by the above analysis, we develop a re-distillation approach to create dataset with high sample effects. This method involves distilling the best-performing RL model (long-CoT) back to the Qwen2.5-1.5B base model. We choose base model rather than initial policy in order to fairly compare its performance with SFTed models. We call it ‘re-distillation’ because we distill target policy again and go back to train base model.

On K&K dataset, we generate responses using the 125-step long-CoT-kk checkpoint, yielding 689 valid samples (re-distill-sft-kk) after correctness and length filtering. Since the SFT puzzles in long-CoT-kk consists of $N_{ppl} = \{2, 3\}$ only, we fine-tune re-distill-rl-kk with RL training samples ($N_{ppl} \in \{3, 4, 5, 6, 7\}$) to fully match data distributions. We randomly select 1K samples from RL training set and re-distill the same checkpoint to get re-distill-rl-kk. The notation of -rl- and -sft- represents the source dataset which we re-distill from but not the training method. Similarly, on MATH dataset, we create the 496-sample re-distill-sft-math dataset from the near-convergence 50-step long-CoT-math checkpoint, which maintains R1-style outputs. Since both the SFT set and RL set on MATH are sampled from original dataset, re-distillation from SFT set fully matches the data distribution.

As shown in Figure 3, **re-distilled models demonstrate accelerated convergence and superior accuracy**. The re-distill-sft-math model attains 54.4% accuracy on MATH-500 while Qwen2.5-1.5B Instruct model achieves 55.0%, with only a gap of 0.6%. On K&K, long-CoT-kk reaches 82.0% accuracy after 125 steps of RL, while re-distill-rl-kk achieves 78.8% through SFT alone. The performance of re-distill-rl-kk achieves 82.0% when evaluated with 8192 max tokens, surpassing DeepSeek-V3-0324 without RL. The Re-distilled model gain small improvement in RL stage, re-distill-rl-kk improved to 84.4%(+2.4 points) after 25 steps’ RL fine-tuning, which outperforms Deepseek-R1-Qwen-Distill-14B(82.0%).

Re-distillation boosts RL efficiency. Re-distillation also leads to better convergence as re-distill-sft-kk reaches 80.2% test accuracy within 25 steps, showing 5 \times higher efficiency than long-CoT-kk with fewer SFT samples ($689 < 763$). The performance gap be-

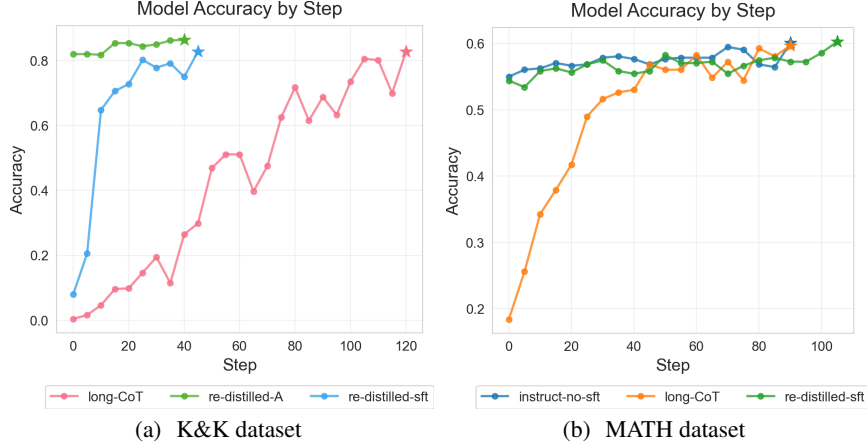


Fig. 3. **Re-distillation matches RL performance through SFT alone** On MATH, re-distill-sft-math matches Qwen2.5-Instruct with only 496 samples. On K&K, re-distill-rl-kk approaches optimal performance without RL, while re-distill-sft-kk converges significantly faster than long-CoT-kk.

tween re-distill-sft-kk and re-distill-rl-kk may due to the dataset distribution shift. re-distill-sft-kk uses simpler data which does not align with RL training set.

6.1 Experimental Verifications

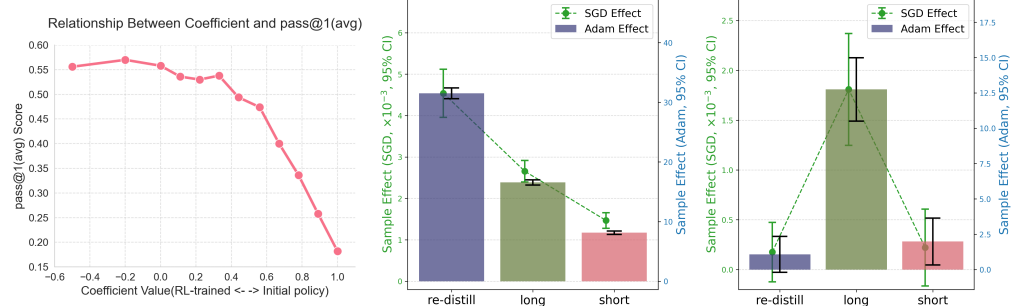


Fig. 4. **Left:** Test accuracy smoothly changes when interpolating from long-CoT-math initial policy to 50-step checkpoint. **Middle:** Average sample effect(dashed green: SGD effect, bar: Adam effect, error bar: 95% CI) of different SFT dataset measured on Qwen2.5-1.5B base. For each SFT model, we randomly select 500 samples from training set. **Right:** Average sample effect of rollout samples measured on RL initial policies(SFTed model). For each model, we randomly select 2000 samples from replay buffer within 4 steps.

We perform further investigation to verify if the effectiveness of re-distillation can be explained by boosted sample effect.

RL has smooth loss landscapes. A key requirement for successful re-distillation is a smooth RL optimization landscape. We analyze this through parameter space interpolation between initial ($\pi(\theta_{old})$) and RL-optimized ($\pi(\theta)$) policies, constructing intermediate models $\pi(\theta_\lambda) = \pi(\lambda\theta_{old} + (1 - \lambda)\theta)$ for $\lambda \in [0, 1]$. Figure 4(left) demonstrates remarkably smooth accuracy transitions. This suggests the feasibility of approximating RL improvements without precisely replicating its gradient trajectory.

Estimated sample effect matches training performance. According to Equation 3 and Equation 4, better sample effect should lead to higher training efficiency. We verify this by computing sample effects from its definition. Specifically, we use normed parameter delta $\Delta\theta = \theta_{25} - \theta_0$ between

Qwen2.5-1.5B base θ_0 and base-no-sft-math 25-step checkpoints θ_{25} to estimate the policy gradient $\mathbb{E}_{s \sim D_e, a \sim \pi_\theta} [\vec{\nabla}_\theta \ln \pi_\theta(a, s) r(a, s)]$. Although it is straight forward to compute policy gradient by its definition, we need an unbiased reference to compare dataset effect for different experiments. The parameter delta is also effective enough because base-no-sft-math shows rapid accuracy growth within 25 steps, which guarantees valid information in $\Delta\theta$.

Specifically, we compute sample effect under both SGD and Adam settings. The SGD sample effect is defined in Definition 5.1. Adam sample effect replaces the last gradient term according to Adam optimizer (Kingma, 2014). Refer to Appendix E for more details. In Figure 4(Middle), we show the estimated SFT effectiveness on different dataset. Re-distilled data of re-distill-sft-math shows 2x efficiency than long CoT data(long-CoT-math). This explains why re-distillation has such superior effect. However, this method failed to predict the correct effect between long CoT and short CoT, it is probably because models have very long response length after distilling from DeepSeek-R1 and tend to exceed max response length in evaluation.

We also compute the sample effect for each initial policy in RL experiments. We compute dataset effect based on initial policy(i.e. SFTed model) to verify the growth rate of test accuracy in initial steps of RL. In Figure 4(Right), long-CoT-math shows the highest RL efficiency, which matches the real performance in subsection 4.2. Notably, re-distill-sft-math has low sample effect because the model is almost converged at the beginning.

6.2 Why SFT Affects Long-Term Exploration

Previous hypothetical analysis only explains how SFT influence RL in initial steps. It remains a question that why RL can not get rid of initial output modes by exploration. We try to explain this by sequential credit assignment. When framing auto-regression as a sequential decision problem, early tokens face ambiguous credit assignment until later tokens approach optimum. For instance, deep reasoning behavior gain little competitive advantage unless LLM learned to generate stop tokens. Hence, initial tokens may converge slower than subsequent ones.

To test this hypothesis, we analyze position-wise logprobs in response tokens. Using initial policy, we evaluate token probabilities across different RL training steps. We compute the 1% lowest logprobs per position as indicators for backward information propagation. Aggregating these measurements reveals a clear pattern in Figure 5(Left): as RL progresses, the token position of the lowest probability point moves from terminal to initial tokens. Notably, terminal tokens exhibit rising probabilities in the converged policy, demonstrating **RL’s tendency to redistribute uncertainty from final to initial tokens**.

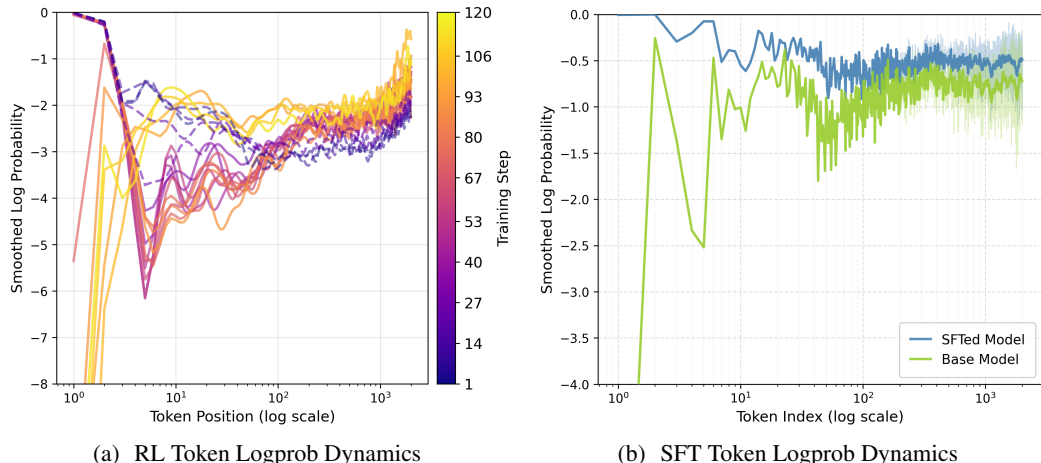


Fig. 5. Divergent Exploration Patterns in RL and SFT. Left: Position-wise logprobs from long-CoT-math RL rollouts evaluated by its initial policy. Right: Logprob distributions before/after SFT on identical data, evaluated by SFTed model of long-CoT-math.

For contrast, we examine pre-/post-SFT logprob distributions across response positions. Figure 5(Right) reveals that SFT induces substantially larger shifts in early tokens. This effect only achieves by RL when it is near convergence. Later tokens show similar trends in both pre-/post-SFT models, suggesting their distributions are shaped through in-context learning. **This demonstrates RL’s inherent difficulty in modifying initial token distributions compared to SFT**, highlighting SFT’s importance for effective exploration.

We further investigate the effect of randomness. We rerun long-CoT-math with an elevated RL temperature and received similar learning trajectories, suggesting simply increase stochasticity cannot substitute SFT’s exploration benefits. See subsection G.1 for details.

7 Experiments Results

We report the main results for all experiments in Table 1 and Table 2. The detailed reward curves are depicted in Appendix G. Refer to subsection C.1 for all experiment settings.

Table 1. Test accuracy in K&K dataset

Model/ N_{ppl}	4	5	6	7	8	Average
Deepseek-R1	0.99	0.99	0.95	0.96	0.95	0.968
Logic-RL-7B [‡]	0.94	0.92	0.91	0.80	0.67	0.848
Deepseek-R1-Qwen-Distill-32B	0.95	0.91	0.85	0.87	0.79	0.874
Deepseek-V3-0324	0.85	0.84	0.86	0.81	0.68	0.808
Deepseek-R1-Qwen-Distill-14B	0.92	0.84	0.81	0.82	0.71	0.820
Deepseek-R1-Qwen-Distill-7B	0.32	0.28	0.12	0.14	0.02	0.176
Qwen-2.5-32B-Instruct	0.41	0.38	0.19	0.15	0.15	0.256
Qwen-2.5-7B-Instruct	0.18	0.17	0.01	0.05	0.01	0.084
Qwen-2.5-1.5B-Instruct	0.03	0.05	0	0.01	0	0.018
w/ long CoT RL	0.49	0.42	0.29	0.18	0.20	0.316
Qwen-2.5-1.5B-Base	0.03	0.01	0.01	0	0	0.010
w/ long CoT SFT	0.01	0	0	0	0	0.002
w/ long CoT SFT + RL	0.91	0.92	0.84	0.78	0.65	0.820
w/ DeepSeek-R1 distillation [†]	0.31	0.25	0.13	0.07	0.09	0.170
w/ Re-distillation[†]	0.94	0.90	0.83	0.74	0.69	0.820
w/ Re-distillation + RL[†]	0.97	0.91	0.85	0.80	0.69	0.844

[‡]: This result is collected from paper. We share identical test set with Logic-RL.

[†]: We use $L_{max} = 8192$ in these models’ evaluation.

Table 2. Test accuracy in MATH-500 dataset

Model	SFT samples	pass@1	pass@1	pass@1
		(0 step)	w/ SFT+RL(100 step)	w/ SFT+RL(final)
instruct-no-sft	-	0.550	0.598	0.604 (150step)
long-CoT	690	0.184	0.554	0.580 (150step)
short-CoT	900	0.298	0.530	-
base-no-sft	-	0.238	0.582	-
re-distill-sft	496	0.544	0.586	0.604 (150 step)
distill-50k	50k	0.278	0.546	0.572 (300 step)
long-CoT-temp1.5	690	0.184	0.584	-
long-CoT-hyperfit	690	0.426	0.416	-

8 Discussion & Conclusion

Limitations and future directions: This study presents several limitations. Firstly, linearized sample effect may not be able to fully explain the non-linear effect in SFT and RL. Secondly, re-distillation is

a post-hoc method which requires RL-trained policy. It remains a problem to select effective samples before SFT or RL. Future research can leverage more advanced method to overcome the limitation of linearized sample effect.

Conclusion: In this work, we investigate the mechanisms behind R1-style Reinforcement Learning (RL) and demonstrate that small-scale Supervised Fine-Tuning (SFT) can achieve comparable performance to RL when using specific dataset. Theoretical and empirical analysis reveal that sample effect is a key indicator of model improvement, explaining why RL-trained policies yield effective distillation data. This work not only explained the success of R1-style RL but also provides a practical framework for improving data efficiency in LLM fine-tuning.

9 Acknowledgement

This work is funded by Noncommunicable Chronic Diseases-National Science and Technology Major Project(Grant No. 2024ZD0522702)

References

Sanjeev Arora, Simon S Du, Wei Hu, Zhiyuan Li, Russ R Salakhutdinov, and Ruosong Wang. On exact computation with an infinitely wide neural net. *Advances in neural information processing systems*, 32, 2019.

Mohammad Gheshlaghi Azar, Zhaohan Daniel Guo, Bilal Piot, Remi Munos, Mark Rowland, Michal Valko, and Daniele Calandriello. A general theoretical paradigm to understand learning from human preferences. In *International Conference on Artificial Intelligence and Statistics*, pages 4447–4455. PMLR, 2024.

Nicholas Carlini, Daphne Ippolito, Matthew Jagielski, Katherine Lee, Florian Tramer, and Chiyuan Zhang. Quantifying memorization across neural language models. In *The Eleventh International Conference on Learning Representations*, 2022.

Fredrik Carlsson, Fangyu Liu, Daniel Ward, Murathan Kurfali, and Joakim Nivre. The Hyperfitting Phenomenon: Sharpening and Stabilizing LLMs for Open-Ended Text Generation. *arXiv preprint arXiv:2412.04318*, 2024.

Ethan Chern, Haoyang Zou, Xuefeng Li, Jiewen Hu, Kehua Feng, Junlong Li, and Pengfei Liu. Generative AI for Math: Abel, 2023. URL <https://github.com/GAIR-NLP/abel>. Publication Title: GitHub repository.

Tianzhe Chu, Yuexiang Zhai, Jihan Yang, Shengbang Tong, Saining Xie, Dale Schuurmans, Quoc V Le, Sergey Levine, and Yi Ma. Sft memorizes, rl generalizes: A comparative study of foundation model post-training. *arXiv preprint arXiv:2501.17161*, 2025.

Kawin Ethayarajh, Winnie Xu, Niklas Muennighoff, Dan Jurafsky, and Douwe Kiela. Kto: Model alignment as prospect theoretic optimization. *arXiv preprint arXiv:2402.01306*, 2024.

Hugging Face. Open R1: A fully open reproduction of DeepSeek-R1, January 2025. URL <https://github.com/huggingface/open-r1>.

Kanishk Gandhi, Ayush Chakravarthy, Anikait Singh, Nathan Lile, and Noah D Goodman. Cognitive behaviors that enable self-improving reasoners, or, four habits of highly effective stars. *arXiv preprint arXiv:2503.01307*, 2025.

Aaron Grattafiori, Abhimanyu Dubey, Abhinav Jauhri, Abhinav Pandey, Abhishek Kadian, Ahmad Al-Dahle, Aiesha Letman, Akhil Mathur, Alan Schelten, Alex Vaughan, and others. The llama 3 herd of models. *arXiv preprint arXiv:2407.21783*, 2024.

Daya Guo, Dejian Yang, Haowei Zhang, Junxiao Song, Ruoyu Zhang, Runxin Xu, Qihao Zhu, Shirong Ma, Peiyi Wang, Xiao Bi, and others. Deepseek-r1: Incentivizing reasoning capability in llms via reinforcement learning. *arXiv preprint arXiv:2501.12948*, 2025.

Valentin Hartmann, Anshuman Suri, Vincent Bindschaedler, David Evans, Shruti Tople, and Robert West. SoK: Memorization in General-Purpose Large Language Models, 2023. URL <https://arxiv.org/abs/2310.18362>. *_eprint*: 2310.18362.

Dan Hendrycks, Collin Burns, Saurav Kadavath, Akul Arora, Steven Basart, Eric Tang, Dawn Song, and Jacob Steinhardt. Measuring mathematical problem solving with the math dataset. *arXiv preprint arXiv:2103.03874*, 2021.

Jian Hu. Reinforce++: A simple and efficient approach for aligning large language models. *arXiv preprint arXiv:2501.03262*, 2025.

Arthur Jacot, Franck Gabriel, and Clément Hongler. Neural tangent kernel: Convergence and generalization in neural networks. *Advances in neural information processing systems*, 31, 2018.

Haozhe Ji, Cheng Lu, Yilin Niu, Pei Ke, Hongning Wang, Jun Zhu, Jie Tang, and Minlie Huang. Towards efficient exact optimization of language model alignment. *arXiv preprint arXiv:2402.00856*, 2024.

Kimi Team, Angang Du, Bofei Gao, Bowei Xing, Changjiu Jiang, Cheng Chen, Cheng Li, Chenjun Xiao, Chenzhuang Du, Chonghua Liao, and others. Kimi k1.5: Scaling reinforcement learning with llms. *arXiv preprint arXiv:2501.12599*, 2025.

Diederik P Kingma. Adam: A method for stochastic optimization. *arXiv preprint arXiv:1412.6980*, 2014.

Woosuk Kwon, Zhuohan Li, Siyuan Zhuang, Ying Sheng, Lianmin Zheng, Cody Hao Yu, Joseph Gonzalez, Hao Zhang, and Ion Stoica. Efficient memory management for large language model serving with pagedattention. In *Proceedings of the 29th Symposium on Operating Systems Principles*, pages 611–626, 2023.

Jia LI, Edward Beeching, Lewis Tunstall, Ben Lipkin, Roman Soletskyi, Shengyi Costa Huang, Kashif Rasul, Longhui Yu, Albert Jiang, Ziju Shen, Zihan Qin, Bin Dong, Li Zhou, Yann Fleureau, Guillaume Lample, and Stanislas Polu. NuminaMath, 2024. Publication Title: Hugging Face repository Published: [<https://huggingface.co/AI-MO/NuminaMath-1.5>](https://github.com/project-numina/aimo-progress-prize/blob/main/report/numina_dataset.pdf).

Xuefeng Li, Haoyang Zou, and Pengfei Liu. Limr: Less is more for rl scaling. *arXiv preprint arXiv:2502.11886*, 2025.

Niklas Muennighoff, Zitong Yang, Weijia Shi, Xiang Lisa Li, Li Fei-Fei, Hannaneh Hajishirzi, Luke Zettlemoyer, Percy Liang, Emmanuel Candès, and Tatsunori Hashimoto. s1: Simple test-time scaling. *arXiv preprint arXiv:2501.19393*, 2025.

OpenAI, Aaron Jaech, Adam Kalai, Adam Lerer, Adam Richardson, Ahmed El-Kishky, Aiden Low, Alec Helyar, Aleksander Madry, Alex Beutel, Alex Carney, Alex Iftimie, Alex Karpenko, Alex Tachard Passos, Alexander Neitz, Alexander Prokofiev, Alexander Wei, Allison Tam, Ally Bennett, Ananya Kumar, Andre Saraiva, Andrea Vallone, Andrew Duberstein, Andrew Kondrich, Andrey Mishchenko, Andy Applebaum, Angela Jiang, Ashvin Nair, Barret Zoph, Behrooz Ghorbani, Ben Rossen, Benjamin Sokolowsky, Boaz Barak, Bob McGrew, Borys Minaiev, Botao Hao, Bowen Baker, Brandon Houghton, Brandon McKinzie, Brydon Eastman, Camillo Lugaresi, Cary Bassin, Cary Hudson, Chak Ming Li, Charles de Bourcy, Chelsea Voss, Chen Shen, Chong Zhang, Chris Koch, Chris Orsinger, Christopher Hesse, Claudia Fischer, Clive Chan, Dan Roberts, Daniel Kappler, Daniel Levy, Daniel Selsam, David Dohan, David Farhi, David Mely, David Robinson, Dimitris Tsipras, Doug Li, Dragos Oprica, Eben Freeman, Eddie Zhang, Edmund Wong, Elizabeth Proehl, Enoch Cheung, Eric Mitchell, Eric Wallace, Erik Ritter, Evan Mays, Fan Wang, Felipe Petroski Such, Filippo Raso, Florencia Leoni, Foivos Tsimpourlas, Francis Song, Fred von Lohmann, Freddie Sulit, Geoff Salmon, Giambattista Parascandolo, Gildas Chabot, Grace Zhao, Greg Brockman, Guillaume Leclerc, Hadi Salman, Haiming Bao, Hao Sheng, Hart Andrin, Hessam Bagherinezhad, Hongyu Ren, Hunter Lightman, Hyung Won Chung, Ian Kivlichan, Ian O’Connell, Ian Osband, Ignasi Clavera Gilabert, Ilge Akkaya, Ilya Kostrikov, Ilya Sutskever, Irina Kofman, Jakub Pachocki, James Lennon, Jason Wei, Jean Harb, Jerry Twore, Jiacheng Feng, Jiahui Yu, Jiayi Weng, Jie Tang, Jieqi Yu, Joaquin Quiñonero Candela, Joe Palermo, Joel Parish,

Johannes Heidecke, John Hallman, John Rizzo, Jonathan Gordon, Jonathan Uesato, Jonathan Ward, Joost Huizinga, Julie Wang, Kai Chen, Kai Xiao, Karan Singhal, Karina Nguyen, Karl Cobbe, Katy Shi, Kayla Wood, Kendra Rimbach, Keren Gu-Lemberg, Kevin Liu, Kevin Lu, Kevin Stone, Kevin Yu, Lama Ahmad, Lauren Yang, Leo Liu, Leon Maksin, Leyton Ho, Liam Fedus, Lilian Weng, Linden Li, Lindsay McCallum, Lindsey Held, Lorenz Kuhn, Lukas Kondraciuk, Lukasz Kaiser, Luke Metz, Madelaine Boyd, Maja Trebacz, Manas Joglekar, Mark Chen, Marko Tintor, Mason Meyer, Matt Jones, Matt Kaufer, Max Schwarzer, Meghan Shah, Mehmet Yatbaz, Melody Y. Guan, Mengyuan Xu, Mengyuan Yan, Mia Glaese, Mianna Chen, Michael Lampe, Michael Malek, Michele Wang, Michelle Fradin, Mike McClay, Mikhail Pavlov, Miles Wang, Mingxuan Wang, Mira Murati, Mo Bavarian, Mostafa Rohaninejad, Nat McAleese, Neil Chowdhury, Neil Chowdhury, Nick Ryder, Nikolas Tezak, Noam Brown, Ofir Nachum, Oleg Boiko, Oleg Murk, Olivia Watkins, Patrick Chao, Paul Ashbourne, Pavel Izmailov, Peter Zhokhov, Rachel Dias, Rahul Arora, Randall Lin, Rapha Gontijo Lopes, Raz Gaon, Reah Miyara, Reimar Leike, Renny Hwang, Rhythm Garg, Robin Brown, Roshan James, Rui Shu, Ryan Cheu, Ryan Greene, Saachi Jain, Sam Altman, Sam Toizer, Sam Toyer, Samuel Miserendino, Sandhini Agarwal, Santiago Hernandez, Sasha Baker, Scott McKinney, Scottie Yan, Shengjia Zhao, Shengli Hu, Shibani Santurkar, Shraman Ray Chaudhuri, Shuyuan Zhang, Siyuan Fu, Spencer Papay, Steph Lin, Suchir Balaji, Suvansh Sanjeev, Szymon Sidor, Tal Broda, Aidan Clark, Tao Wang, Taylor Gordon, Ted Sanders, Tejal Patwardhan, Thibault Sottiaux, Thomas Degry, Thomas Dimson, Tianhao Zheng, Timur Garipov, Tom Stasi, Trapit Bansal, Trevor Creech, Troy Peterson, Tyna Eloundou, Valerie Qi, Vineet Kosaraju, Vinnie Monaco, Vitchyr Pong, Vlad Fomenko, Weiyi Zheng, Wenda Zhou, Wes McCabe, Wojciech Zaremba, Yann Dubois, Yinghai Lu, Yining Chen, Young Cha, Yu Bai, Yuchen He, Yuchen Zhang, Yunyun Wang, Zheng Shao, and Zhuohan Li. OpenAI o1 System Card, 2024. URL <https://arxiv.org/abs/2412.16720>. _eprint: 2412.16720.

OpenAI, Ahmed El-Kishky, Alexander Wei, Andre Saraiva, Borys Minaiev, Daniel Selsam, David Dohan, Francis Song, Hunter Lightman, Ignasi Clavera, Jakub Pachocki, Jerry Tworek, Lorenz Kuhn, Lukasz Kaiser, Mark Chen, Max Schwarzer, Mostafa Rohaninejad, Nat McAleese, o3 contributors, Oleg Mürk, Rhythm Garg, Rui Shu, Szymon Sidor, Vineet Kosaraju, and Wenda Zhou. Competitive Programming with Large Reasoning Models, 2025. URL <https://arxiv.org/abs/2502.06807>. _eprint: 2502.06807.

Qwen Team. QwQ-32B: Embracing the Power of Reinforcement Learning, March 2025. URL <https://qwenlm.github.io/blog/qwq-32b/>.

Rafael Rafailov, Archit Sharma, Eric Mitchell, Christopher D Manning, Stefano Ermon, and Chelsea Finn. Direct preference optimization: Your language model is secretly a reward model. *Advances in Neural Information Processing Systems*, 36:53728–53741, 2023.

Yi Ren and Danica J Sutherland. Learning dynamics of llm finetuning. *arXiv preprint arXiv:2407.10490*, 2024.

Guangming Sheng, Chi Zhang, Zilingfeng Ye, Xibin Wu, Wang Zhang, Ru Zhang, Yanghua Peng, Haibin Lin, and Chuan Wu. Hybridflow: A flexible and efficient rlhf framework. *arXiv preprint arXiv:2409.19256*, 2024.

Richard S Sutton, David McAllester, Satinder Singh, and Yishay Mansour. Policy Gradient Methods for Reinforcement Learning with Function Approximation. In S. Solla, T. Leen, and K. Müller, editors, *Advances in Neural Information Processing Systems*, volume 12. MIT Press, 1999. URL https://proceedings.neurips.cc/paper_files/paper/1999/file/464d828b85b0bed98e80ade0a5c43b0f-Paper.pdf.

Jason Wei, Xuezhi Wang, Dale Schuurmans, Maarten Bosma, Fei Xia, Ed Chi, Quoc V Le, Denny Zhou, and others. Chain-of-thought prompting elicits reasoning in large language models. *Advances in neural information processing systems*, 35:24824–24837, 2022.

Chulin Xie, Yangsibo Huang, Chiyuan Zhang, Da Yu, Xinyun Chen, Bill Yuchen Lin, Bo Li, Badih Ghazi, and Ravi Kumar. On memorization of large language models in logical reasoning. *arXiv preprint arXiv:2410.23123*, 2024.

Tian Xie, Zitian Gao, Qingnan Ren, Haoming Luo, Yuqian Hong, Bryan Dai, Joey Zhou, Kai Qiu, Zhirong Wu, and Chong Luo. Logic-rl: Unleashing llm reasoning with rule-based reinforcement learning. *arXiv preprint arXiv:2502.14768*, 2025.

An Yang, Baosong Yang, Beichen Zhang, Binyuan Hui, Bo Zheng, Bowen Yu, Chengyuan Li, Dayiheng Liu, Fei Huang, Haoran Wei, and others. Qwen2. 5 technical report. *arXiv preprint arXiv:2412.15115*, 2024a.

An Yang, Beichen Zhang, Binyuan Hui, Bofei Gao, Bowen Yu, Chengpeng Li, Dayiheng Liu, Jianhong Tu, Jingren Zhou, Junyang Lin, and others. Qwen2. 5-math technical report: Toward mathematical expert model via self-improvement. *arXiv preprint arXiv:2409.12122*, 2024b.

Yixin Ye, Zhen Huang, Yang Xiao, Ethan Chern, Shijie Xia, and Pengfei Liu. LIMO: Less is More for Reasoning. *arXiv preprint arXiv:2502.03387*, 2025.

Edward Yeo, Yuxuan Tong, Morry Niu, Graham Neubig, and Xiang Yue. Demystifying long chain-of-thought reasoning in llms, 2025. URL <https://arxiv.org/pdf/2502.03373.pdf>, 2025.

Qiyi Yu, Zheng Zhang, Ruofei Zhu, Yufeng Yuan, Xiaochen Zuo, Yu Yue, Tiantian Fan, Gaohong Liu, Lingjun Liu, Xin Liu, and others. Dapo: An open-source llm reinforcement learning system at scale. *arXiv preprint arXiv:2503.14476*, 2025.

Weihao Zeng, Yuzhen Huang, Qian Liu, Wei Liu, Keqing He, Zejun Ma, and Junxian He. Simplerl-zoo: Investigating and taming zero reinforcement learning for open base models in the wild. *arXiv preprint arXiv:2503.18892*, 2025.

Rosie Zhao, Alexandru Meterez, Sham Kakade, Cengiz Pehlevan, Samy Jelassi, and Eran Malach. Echo chamber: RL post-training amplifies behaviors learned in pretraining. *arXiv preprint arXiv:2504.07912*, 2025.

A Proofs

Assumptions in this paper

1. Our core assumption is: linearized sample effect is able to explain the effectiveness of multi-step and non-linear LLM training process.
2. To analyze discrete gradient decent with SDE, learning rate η should be sufficiently small.
3. N is sufficiently large to apply Central Limit Theorem.
4. In initial steps of RL, by setting suitable hyperparameters, we can approximate drift term by ignoring the noise effect.

A.1 Proof of Instantaneous Growth Rate of Accuracy

We start from the policy gradient loss:

$$-\nabla_{\theta} L = \frac{1}{N} \sum_{a \sim \pi_{\theta}, s \sim D_t} [\vec{\nabla}_{\theta} \ln \pi_{\theta}(a, s) r(a, s)] \quad (7)$$

By Central Limit Theorem, we can represent the estimation noise by Wiener Process.

$$d\theta = \mathbb{E}_{a \sim \pi_{\theta}, s \sim D_t} [\vec{\nabla}_{\theta} \ln \pi_{\theta}(a, s) r(a, s)] dt + \sqrt{\frac{\eta}{N}} \mathbf{A} d\vec{W}_t \quad (8)$$

The matrix \mathbf{A} satisfies:

$$\mathbf{A} \mathbf{A}^T = \text{Cov}_{s \sim D_t, a \sim \pi_{\theta}} [r(a, s) \partial / \partial \theta_i \ln \pi_{\theta}(a, s), r(a, s) \partial / \partial \theta_j \ln \pi_{\theta}(a, s)] \quad (9)$$

Let \vec{A}_i denotes the i -th column in \mathbf{A} . W_i denotes the i -th component of \vec{W}_t . We can re-write Equation 8 as:

$$d\theta = \mathbb{E}_{s \sim D_t, a \sim \pi_\theta} [\vec{\nabla}_\theta \ln \pi_\theta(a, s) r(a, s)] dt + \sqrt{\frac{\eta}{N}} \sum_{i=1}^n \vec{A}_i dW_i \quad (10)$$

We define the growth rate of test reward(accuracy) in time t as $\Psi(\theta(t))$:

$$\Psi(\theta) = \mathbb{E}_{a \sim \pi_\theta, s \sim D_e} [r(a, s)] \quad (11)$$

For a standard SDE $d\vec{X} = \vec{f}(\vec{X}, t)dt + \sum_{i=1}^n \vec{g}_i(\vec{X}, t)dW_i$, we can compute any $\Psi(\vec{X})$ using Ito's lemma:

$$d\Psi(\vec{X}) = \mu(t, \vec{X})dt + \sigma(t, \vec{X})d\vec{W}_t \quad (12)$$

$$= \underbrace{[\vec{\nabla}_X \Psi]^\top \vec{f}(\vec{X})dt + \frac{1}{2} \sum_{i=1}^n \vec{g}_i(\vec{X})^\top \nabla^2 \Psi(\vec{X}) \vec{g}_i(\vec{X})dt}_{\text{Drift term}} \quad (13)$$

$$+ \underbrace{\sum_{i=1}^n [\vec{\nabla}_X \Psi]^\top \vec{g}_i(\vec{X})dW_i}_{\text{Noise term}} \quad (14)$$

We derive drift term by substituting variables in the first and second terms.

$$\mu(t, \Psi(\theta)) = \mathbb{E}_{s \sim D_e, a \sim \pi_\theta} [\vec{\nabla}_\theta \ln \pi_\theta(a, s) r(a, s)]^\top \mathbb{E}_{s \sim D_t, a \sim \pi_\theta} [\vec{\nabla}_\theta \ln \pi_\theta(a, s) r(a, s)] \quad (15)$$

$$+ \frac{1}{2} \frac{\eta}{N} \sum_{i=1}^n \vec{A}_i^T \nabla^2 \Psi(\vec{X}) \vec{A}_i \quad (16)$$

A.2 Proof of Theorem 5.1

The proof of Theorem 5.1 is similar to DPO (Rafailov et al., 2023). Let $\pi_\theta^\dagger(a, s)$ to be the target policy. $\hat{\pi}_\theta^\dagger(a, s)$ to be the distribution after correctness filter. We have $\hat{\pi}_\theta^\dagger(a, s) = \frac{\pi_\theta^\dagger(a, s)}{p_\theta^\dagger(s)} r(a, s)$. We find $\pi_\theta^\dagger(a, s)$, which satisfies $\mathbb{E}_{s \sim D_t, a \sim \pi_\theta^\dagger} [r(a, s)] = p_\theta^\dagger(s)$, to maximize the objective \mathcal{J} .

$$\mathcal{J} = \mathbb{E}_{s \sim D_t, a \sim \hat{\pi}_\theta^\dagger} [V(a, s, \theta) r(a, s)] - \mathbb{E}_{s \sim D_t, a \sim \pi_\theta} [V(a, s, \theta) r(a, s)] \quad (17)$$

$$- \beta \mathbb{D}_{KL}[\pi_\theta^\dagger(a, s) || \pi_\theta(a, s)] \quad (18)$$

$$V(a, s, \theta) = \mathbb{E}_{s \sim D_e, a \sim \pi_\theta} [\vec{\nabla}_\theta \ln \pi_\theta(a, s) r(a, s)]^\top \vec{\nabla}_\theta \ln \pi_\theta(a, s) \quad (19)$$

$$\hat{\pi}_\theta^\dagger(a, s) = \frac{\pi_\theta^\dagger(a, s)}{p_\theta^\dagger(s)} r(a, s) \quad (20)$$

$$p_\theta^\dagger(s) = \mathbb{E}_{s \sim D_t, a \sim \pi_\theta^\dagger} [r(a, s)] \quad (21)$$

$$\mathbb{D}_{KL}[\hat{\pi}_\theta^\dagger(a, s) || \pi_\theta(a, s)] = \mathbb{E}_{s \sim D_t, a \sim \hat{\pi}_\theta^\dagger} [\ln \frac{\hat{\pi}_\theta^\dagger(a, s)}{\pi_\theta(a, s)}] \quad (22)$$

$$r(a, s) = 1 \text{ if } a \text{ is correct else } 0 \quad (23)$$

The second term of \mathcal{J} does not depend on $\pi_\theta^\dagger(a, s)$. We eliminate the second term and rewrite objective as:

$$\max_{\pi_\theta^\dagger} \mathcal{J} \quad (24)$$

$$= \max_{\pi_\theta^\dagger} \mathbb{E}_{s \sim D_t, a \sim \pi_\theta^\dagger} [V(a, s, \theta) r(a, s)] - \beta \mathbb{D}_{KL}[\pi_\theta^\dagger(a, s) \parallel \pi_\theta(a, s)] \quad (25)$$

$$= \max_{\pi_\theta^\dagger} \mathbb{E}_{s \sim D_t, a \sim \pi_\theta^\dagger} \left[\frac{1}{p_\theta^\dagger(s)} V(a, s, \theta) r(a, s) - \beta \ln \frac{\pi_\theta^\dagger(a, s)}{\pi_\theta(a, s)} \right] \quad (26)$$

$$= \min_{\pi_\theta^\dagger} \mathbb{E}_{s \sim D_t, a \sim \pi_\theta^\dagger} \left[\ln \frac{\pi_\theta^\dagger(a, s)}{Z(a, s)} \pi_\theta(a, s) \exp\left(\frac{1}{\beta p_\theta^\dagger(s)} V(a, s, \theta) r(a, s)\right) - \ln Z(a, s) \right] \quad (27)$$

In the above we use $r(a, s) = r^2(a, s)$. For simplicity, we denote $\hat{r}(a, s, \theta) = \frac{1}{p_\theta^\dagger(s)} V(a, s, \theta) r(a, s)$. Differ from DPO, we define $Z(a, s)$ as:

$$Z(a, s) = \begin{cases} \frac{1}{p_\theta^\dagger(s)} \sum_a r(a, s) \pi_\theta(a, s) \exp\left(\frac{1}{\beta} \hat{r}(a, s, \theta)\right) = Z^+(s) & \text{if } r(a, s) = 1 \\ \frac{1}{1-p_\theta^\dagger(s)} \sum_a (1 - r(a, s)) \pi_\theta(a, s) = Z^-(s) & \text{if } r(a, s) = 0 \end{cases} \quad (28)$$

Then we define $\pi_\theta^*(a, s) = \frac{1}{Z(a, s)} \pi_\theta(a, s) \exp\left(\frac{1}{\beta} \hat{r}(a, s, \theta)\right)$. We have $\pi_\theta^*(a, s) \geq 0$, and we verify it is a valid distribution:

$$\sum_a \pi_\theta^*(a, s) = \sum_a r(a, s) \pi_\theta^*(a, s) + \sum_a (1 - r(a, s)) \pi_\theta^*(a, s) \quad (29)$$

$$= \frac{1}{Z^+(s)} \sum_a r(a, s) \pi_\theta(a, s) \exp\left(\frac{1}{\beta} \hat{r}(a, s, \theta)\right) + \frac{1}{Z^-(s)} \sum_a (1 - r(a, s)) \pi_\theta(a, s) \quad (30)$$

$$= p_\theta^\dagger(s) + (1 - p_\theta^\dagger(s)) \quad (31)$$

$$= 1 \quad (32)$$

We can also check the accuracy constraint is satisfied: $\sum_a r(a, s) \pi_\theta^*(a, s) = p_\theta^\dagger(s)$.

To eliminate $\ln Z(a, s)$, we prove that $\mathbb{E}_{s \sim D_t, a \sim \pi_\theta^\dagger} [\ln Z(a, s)]$ does not depend on π_θ^\dagger :

$$\mathbb{E}_{s \sim D_t, a \sim \pi_\theta^\dagger} [\ln Z(a, s)] = \sum_{s, a} \pi_\theta^\dagger(a, s) \ln Z(a, s) \quad (33)$$

$$= \sum_{s, a} \pi_\theta^\dagger(a, s) r(a, s) \ln Z^+(s) + \sum_{s, a} \pi_\theta^\dagger(a, s) (1 - r(a, s)) \ln Z^-(s) \quad (34)$$

$$= \sum_s [\ln Z^+(s) \sum_a \pi_\theta^\dagger(a, s) r(a, s) + \ln Z^-(s) \sum_a \pi_\theta^\dagger(a, s) (1 - r(a, s))] \quad (35)$$

$$= \sum_s [p_\theta^\dagger(s) \ln Z^+(s) + (1 - p_\theta^\dagger(s)) \ln Z^-(s)] \quad (36)$$

Therefore, we can simplify the last line in Equation 24 and finally get:

$$\max_{\pi_\theta^\dagger} \mathcal{J} = \min_{\pi_\theta^\dagger} \mathbb{E}_{s \sim D_t, a \sim \pi_\theta^\dagger} \left[\ln \frac{\pi_\theta^\dagger(a, s)}{\pi_\theta^*(a, s)} \right] \quad (37)$$

$$= \min_{\pi_\theta^\dagger} \mathbb{D}_{KL}[\pi_\theta^\dagger(a, s) \parallel \pi_\theta^*(a, s)] \quad (38)$$

The KL distance achieves global minimum 0 if and only if $\pi_\theta^\dagger(a, s) = \pi_\theta^*(a, s)$. We prove that $\pi_\theta^*(a, s)$ is the optimal policy.

For any a_1, a_2 and $s \in \{D_t\}$ satisfies $r(a_1, s) = r(a_2, s) = 1$, we have:

$$\ln \frac{\pi_\theta^*(a_1, s)}{\pi_\theta^*(a_2, s)} = \ln \frac{\frac{1}{Z^+(s)} \pi_\theta(a_1, s) \exp(\frac{1}{\beta} \hat{r}(a_1, s, \theta))}{\frac{1}{Z^+(s)} \pi_\theta(a_2, s) \exp(\frac{1}{\beta} \hat{r}(a_2, s, \theta))} \quad (39)$$

$$= \frac{1}{\beta p_\theta^\dagger(s)} (V(a_1, s, \theta) - V(a_2, s, \theta)) + \ln \frac{\pi_\theta(a_1, s)}{\pi_\theta(a_2, s)} \quad (40)$$

To prove Corollary 1, note that for any new $p_\theta^\dagger(s) > 0$, we can always find another β' and $p_\theta'(s)$ to keep $\frac{1}{\beta} \hat{r}(a, s, \theta) = \frac{1}{\beta p_\theta^\dagger(s)} V(a, s, \theta) r(a, s)$ unchanged. The filtered distribution $\hat{\pi}_\theta^\dagger(a, s) = r(a, s) \frac{\pi_\theta(a, s) \exp(\frac{1}{\beta} \hat{r}(a, s, \theta))}{p_\theta^\dagger(s) Z^+(s)}$ contains no single $p_\theta^*(s)$. Therefore, the optimal distribution keep unchanged.

A.3 Proof of Theorem 5.2

Given a policy $\pi_\theta^*(a, s)$ in RL, the distribution after filtering is $\hat{\pi}_\theta^*(a, s)$. We use filtered data to fine-tune initial policy $\pi_\theta(a, s)$. We define dataset effect as:

$$V(\theta, \theta^*, D_t) = \mathbb{E}_{s \sim D_t, a \sim \hat{\pi}_\theta^*} [V(a, s, \theta) r(a, s)] \quad (41)$$

$$= \mathbb{E}_{s \sim D_t, a \sim \pi_\theta^*} \left[\frac{1}{p_\theta^*(s)} V(a, s, \theta) r(a, s) \right] \quad (42)$$

Note that sample effect $V(a, s, \theta)$ and dataset effect $V(\theta, \theta^*, D_t)$ have different input variables. The growth rate of training set dataset effect can be expressed as:

$$\hat{\mu}(t, V(\theta, \theta^*, D_t)) = [\nabla_{\theta^*} V(\theta, \theta^*, D_t)]^\top \mathbb{E}_{s \sim D_t, a \sim \pi_\theta^*} [\nabla_{\theta^*} \ln \pi_\theta^*(a, s) r(a, s)] \quad (43)$$

$$= \mathbb{E}_{s \sim D_t, a \sim \pi_\theta^*} \left[\frac{1}{p_\theta^*(s)} \nabla_{\theta^*} \ln \pi_\theta^*(a, s) V(a, s, \theta) r(a, s) \right]^\top \mathbb{E}_{s \sim D_t, a \sim \pi_\theta^*} [\nabla_{\theta^*} \ln \pi_\theta^*(a, s) r(a, s)] \quad (44)$$

$$= \mathbb{E}_{s \sim D_t, a \sim \pi_\theta^*} \left[\frac{1}{p_\theta^*(s)} V(a, s, \theta^*) V(a, s, \theta) r(a, s) \right] \quad (45)$$

Set $\theta = \theta^*$ to get the instantaneous growth rate of dataset effect. Continue to simplify Equation 43:

$$\hat{\mu}(t, V(\theta, \theta^*, D_t)) = \mathbb{E}_{s \sim D_t, a \sim \pi_\theta} \left[\frac{1}{p_\theta(s)} V^2(a, s, \theta) r(a, s) \right] \quad (46)$$

Since $\frac{1}{p_\theta(s)} \geq 1$ and $r(a, s) = r^2(a, s)$, we have:

$$\hat{\mu}(t, V(\theta, \theta^*, D_t)) \geq \mathbb{E}_{s \sim D_t, a \sim \pi_\theta} [V^2(a, s, \theta) r^2(a, s)] \quad (47)$$

By $E[X^2] \geq E^2[X]$, we have:

$$\hat{\mu}(t, V(\theta, \theta^*, D_t)) \geq \mathbb{E}_{s \sim D_t, a \sim \pi_\theta} [V^2(a, s, \theta) r^2(a, s)] \quad (48)$$

$$\geq \|\mathbb{E}_{s \sim D_t, a \sim \pi_\theta} [V(a, s, \theta) r(a, s)]\|^2 \quad (49)$$

$$= \hat{\mu}^2(t, \Psi(\theta)) \quad (50)$$

B Output mode dynamics during RL training

We provide empirical evaluation of output modes during RL training. To analyze output modes, we classify responses into distinct modes and track their proportions, while monitoring mean accuracy and cumulative advantage for each mode. We describe classification method in Appendix I and show qualitative evaluations in Appendix J.

Output modes undergo rapid transitions following advantage fluctuations. As shown in Figure 6 (Left), we evaluate output modes in long-CoT-kk RL steps. The 'Wait' pattern disappears abruptly between steps 20-40 during an advantage surge, with similar behavior observed on the MATH dataset (right). RL policy may maintain more than one output modes simultaneously. In Figure 6 (Right), we evaluate output modes in long-CoT-math. The short mode persists at approximately 20% even after stabilization.

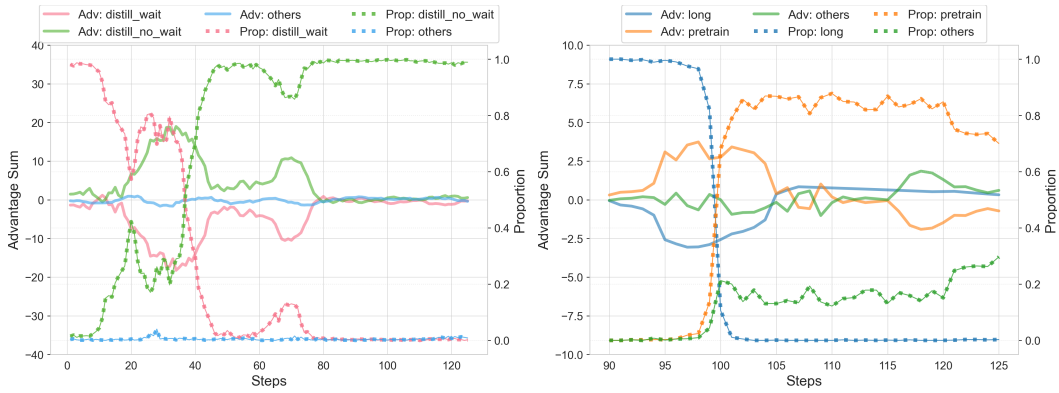


Fig. 6. **Dynamics of output mode transitions** Left: Disappearance of 'Wait' pattern following advantage increase. Right: pretrain mode reflects Qwen-2.5-1.5B's original output patterns, while short mode corresponds to short-CoT-math data style. The pretrained pattern re-emerges after 100 steps as long-CoT-math approaches convergence.

LLM revert to pre-SFT output patterns. The resurgence of pretrain modes in Figure 6(right) suggests that SFT temporarily switches rather than permanently alters base model behavior. These findings indicate that SFT effectiveness depends critically on alignment with the model's intrinsic behavioral patterns, which resist modification through limited fine-tuning.

C Can LLM Progressively Improve Through Stable Reasoning Patterns?

We investigate whether smaller LLMs can achieve progressive self-improvement when maintaining stable reasoning patterns through two approaches: extended SFT and hyperfitting. We show test performances in Table 3 and training statistics in Figure 10.

First, we scale supervised fine-tuning using 50K high-quality reasoning traces from OpenR1-Math-220K, which distills DeepSeek-R1 on NuminaMath 1.5 (Face, 2025; LI et al., 2024). We extract solutions no longer than 16K tokens and randomly pick 50K samples. The SFTed distill-50k-math receives the same training recipe as long-CoT-math. However, distill-50k-math shows worse learning curve than long-CoT-math. While output structure remains stable during training, performance plateaus with reward improvements requiring twice as many steps as baseline models to achieve comparable accuracy.

Second, we implement Hyperfitting (Carlsson et al., 2024; Ye et al., 2025) on long-CoT-math through 15-epoch training, achieving near-zero SFT loss. The long-CoT-hyperfit-math model shows reduced repetition after SFT, but exhibits severely constrained exploration and sub-optimal reward curve during RL.

These experiments demonstrate that **enforcing rigid reasoning patterns impedes RL efficiency**. While both methods successfully stabilize output patterns, neither enables smaller models to surpass

Table 3. Test accuracy in MATH-500 dataset

Model	pass@1 (0 step)	pass@1 w/ SFT+RL(100 step)	pass@1 w/ SFT+RL(final)
instruct-no-sft	0.550	0.598	0.604 (150step)
long-CoT-hyperfit-math	0.426	0.416	-
distill-50k-math	0.278	0.546	0.572 (300 step)

inherent performance ceilings. This limitation may stem from intrinsic model ability which can only be improved by large scale pretraining.

C.1 Experiment settings

We list all Supervised Fine-Tuning, Reinforce Learning and Re-distillation experiments as well as other baselines as follows:

K&K experiments: short-CoT-kk (1K programmatic data) and long-CoT-kk (1K DeepSeek-R1 traces) are fine-tuned with filtered correct solutions no longer than 4096 tokens. We add `base-no-sft` and `instruct-no-sft` from pretrained models as baselines and optimize these four models by GRPO. Then we generate 1K SFT samples with the same prompt from the best policy long-CoT-kk to create `re-distilled-sft-kk`, demonstrating accelerated RL convergence. To show the potential of Re-distillation, we sample 1K filtered samples from RL training set to train `re-distilled-rl-kk`, which matches long-CoT-kk performance without RL. Re-distilled models are trained from Qwen2.5-1.5B base. We prompt DeepSeek-R1 with questions in `re-distilled-rl-kk` and SFT base model to train `baseline-rl-distillation`, which uses the same training recipe. This experiment shows the effect of `re-distilled-rl-kk` comes from re-distillation but not higher difficulty of SFT dataset.

MATH experiments: The four experiments in MATH dataset: short-CoT-math, long-CoT-math, `instruct-no-sft-math` and `base-no-sft-math` are established with similar settings in K&K dataset. We distill long-CoT-math prompted by the same questions in SFT stage to get `re-distill-sft-math`. It is able to directly match long-CoT-math performance without RL.

Hyper-parameter tuning: In K&K experiments, we found setting $\beta_1 = 0.5$ in Adam optimizer enables better RL convergence. We set $\beta_1 = 0.9$ for comparison. See subsection G.2 for results. In subsection 6.2, we set rollout temperature to 1.2 in `long-CoT-math-temp-1.2` and compare results with `long-CoT-math`, which uses temperature 0.7.

More SFT data: We investigate how more SFT data/epochs affect performance in Appendix C. In `hyperfit-math`, we use hyperfit method to fit SFT data in long-CoT-math with 15 epochs then perform RL. In `distill-50k-math`, we SFT Qwen2.5-1.5B Base with 50K data filtered from OpenR1-Math 220K and perform RL.

D Training Details

Our training pipeline implementation is based on VeRL (Sheng et al., 2024) and vLLM (Kwon et al., 2023). We use 2xA800 80G for all experiments.

D.1 Supervised Fine-tuning

In SFT stage, we use Adam optimizer without weight decay. On K&K dataset, we use a batch size of 64, learning rate of 1e-5, cosine scheduler and 5000 token as max length. We train K&K models for 2 epochs except `short-CoT-kk` for 1 epoch because its loss reached near zero within one epoch. For small-scale SFT on MATH dataset, we use a batch size of 32 and keep other settings unchanged. Re-distillation has no difference with SFT in hyper-parameters except `re-distill-rl-kk`. Since the aim of `re-distill-rl-kk` is to exploit information from 1K samples. We use batch size equals to 32 to boost performance.

For Continued PreTraining in `distill-50k-math`, we use batch size of 64, 12K token as max length, 1e-5 learning rate, cosine scheduler and 1 training epoch. We found a larger batch size and lower learning rate make CPT more stable.

D.1.1 Reinforcement Learning

Hyperparameters: We list GRPO configuration as follows.

Rollout: 8 responses per question (temperature=0.7, max length=4096), 128 random selected problems per rollout. Exceptionally, we use max length=8192 for `re-distillation-rl-kk`.

Policy update: Single 1024-sample batch, clip ratio=0.2, gradient norm=1.0

Optimization: Adam ($\beta_1 = 0.5, \beta_2 = 0.999$)

Learning rates: 5.0e-6 (K&K), 2.5e-6 (MATH) with 4 warm-up steps

Other settings: Sequence packing with 15K tokens per batch

Training Algorithm: We adapt GRPO by eliminating the KL divergence constraint, following DAPO’s approach (Yu et al., 2025). To improve RL stability, we set the training batch size equal to the rollout buffer size, ensuring sufficient valid samples per update. Empirical results demonstrate better performance with lower β_1 in Adam optimizer parameters ($\beta_1 = 0.5, \beta_2 = 0.999$), particularly when encountering lengthy outputs that frequently trigger clipping. We conduct ablation experiments for β_1 in Adam optimizer on `long-CoT-kk`, `short-CoT-kk` and `instruct-no-sft-kk`. In Figure 7, all three experiments show consistent improvement by tuning β_1 from 0.9 to 0.5. Therefore, we use this setting in following experiments.

Reward Function: We use binary reward function which only outputs 0 or 1. This reward function requires the end-of-sentence token to give correctness reward. Responses exceeding output length will be assigned to 0 reward despite its correctness. We observed that 1.5B models tend to endlessly repeat final answer and fill the rest token lengths, which prohibits natural response length growth in some cases. This design prevents excessive repetition by requiring an end-of-sentence token. The K&K dataset employs strict matching between extracted name-identity lists and ground truth. The reward function for checking MATH answers is implemented based on Zeng et al. (2025) and Yang et al. (2024b). We slightly modify it to check the answer in final boxed $\{\}$. Both MATH and K&K reward functions assign zero reward to responses exceeding length limits or containing no boxed answers. We exclude format reward to prevent instability and keep simplicity.

E Details in Empirical Verification

We use delta of parameters $\Delta\theta$ as policy gradient approximation. We compute SFT effect with SGD V_{SGD} as described in Equation 51. $|a|$ is the response token length.

$$\vec{g}_t = \frac{1}{N} \sum_{i=1}^N \vec{\nabla}_\theta \ln \pi_\theta(a, s) / |a| \quad (51)$$

$$V_{\text{SGD}} = - \frac{\vec{g}_t}{\|\vec{g}_t\|}^\top \vec{\Delta}\theta \quad (52)$$

We compute SFT effect with Adam (V_{Adam}) by Equation 53.

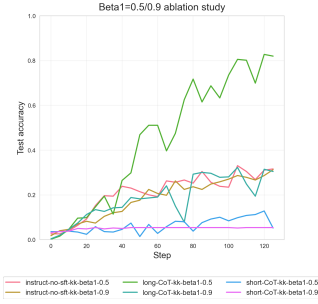


Fig. 7. Test accuracy for hyper-parameter ablation study: $\beta_1 = 0.9$ vs $\beta_1 = 0.5$. We observed that $\beta_1 = 0.9$ shows equal or better performance than $\beta_1 = 0.5$ under three settings.

$$\vec{m}_t = \beta_1 \vec{m}_{t-1} + (1 - \beta_1) \frac{\vec{g}_t}{\|\vec{g}_t\|} \quad (53)$$

$$\vec{v}_t = \beta_2 \vec{v}_{t-1} + (1 - \beta_2) \frac{\vec{g}_t}{\|\vec{g}_t\|} \odot \frac{\vec{g}_t}{\|\vec{g}_t\|} \quad (54)$$

$$\hat{\vec{m}}_t = \frac{\vec{m}_t}{1 - \beta_1^t} \quad (55)$$

$$\hat{\vec{v}}_t = \frac{\vec{v}_t}{1 - \beta_2^t} \quad (56)$$

$$V_{\text{Adam}} = - \left[\frac{\hat{\vec{m}}_t}{\sqrt{\hat{\vec{v}}_t + \epsilon}} \right]^\top \vec{\Delta\theta} \quad (57)$$

We use the following method to compute sample effect in RL. $A(a, s)$ is the advantage function computed in RL. Replace \vec{g}_t in Equation 51 and Equation 53 to compute sample effect with SGD and Adam.

$$\vec{g}_t = \frac{1}{N} \sum_{i=1}^N \nabla_\theta \ln \pi_\theta(a, s) A(a, s) / |a| \quad (58)$$

(59)

F Evaluation Metrics

We evaluate model performance using *pass@1* accuracy on held-out test sets. For R1-distilled models, we employ the recommended configuration from DeepSeek: temperature=0.6, top_p=0.95, and system prompt removal. Other evaluations use greedy decoding. Following Zeng et al. (2025) and Chern et al. (2023), we employ question-answer prompts in `base-no-sft` to mitigate its poor instruction-following capability. See Appendix H for prompt templates. All reported results zero-shot, which may yield minor discrepancies compared to Qwen technical report (Yang et al., 2024b) due to metric differences.

In Table 1, we use 8K max tokens for DeepSeek-V3-0324 and Deepseek-R1-Qwen-Distill-14B/7B. 16K tokens for Deepseek-R1 and Deepseek-R1-Qwen-Distill-32B. 4K tokens for Qwen2.5 Instruct models. The trained model in our experiments are tested with 4096 max tokens except re-distill-rl-kk since we want to compare its performance with the same length as DeepSeek-V3-0324.

G Detailed Reinforcement Learning Statistics

G.1 Ablation study by increasing randomness in RL exploration

We rerun `long-CoT-math` with temperature 1.2. As shown in Figure 8, the test accuracy between `long-CoT-math` and `long-CoT-temp1.2-math` shows similar trends. However, raising temperature significantly influence exploration entropy.

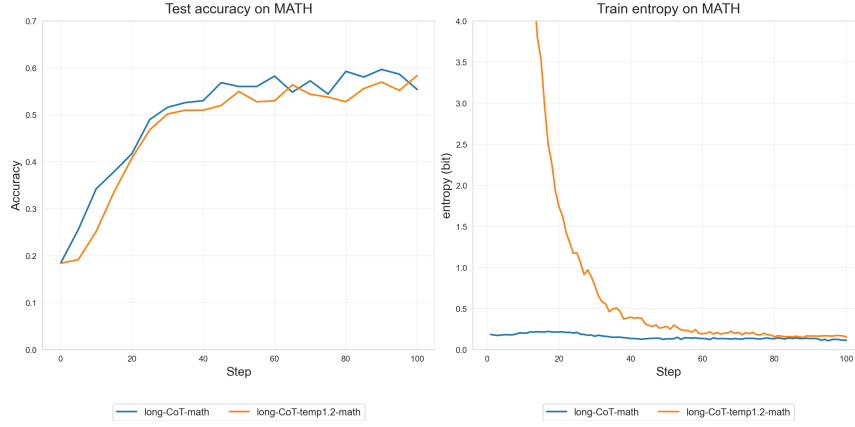


Fig. 8. **Left:** Increasing temperature will not bring substantial improvement. Two models share the same GRPO recipe except different rollout temperatures. **Right:** Increasing temperature leads to significantly higher entropy in initial steps.

G.2 Detailed Statistics on K&K dataset

We list detailed statistics for experiments on K&K dataset in Figure 9.

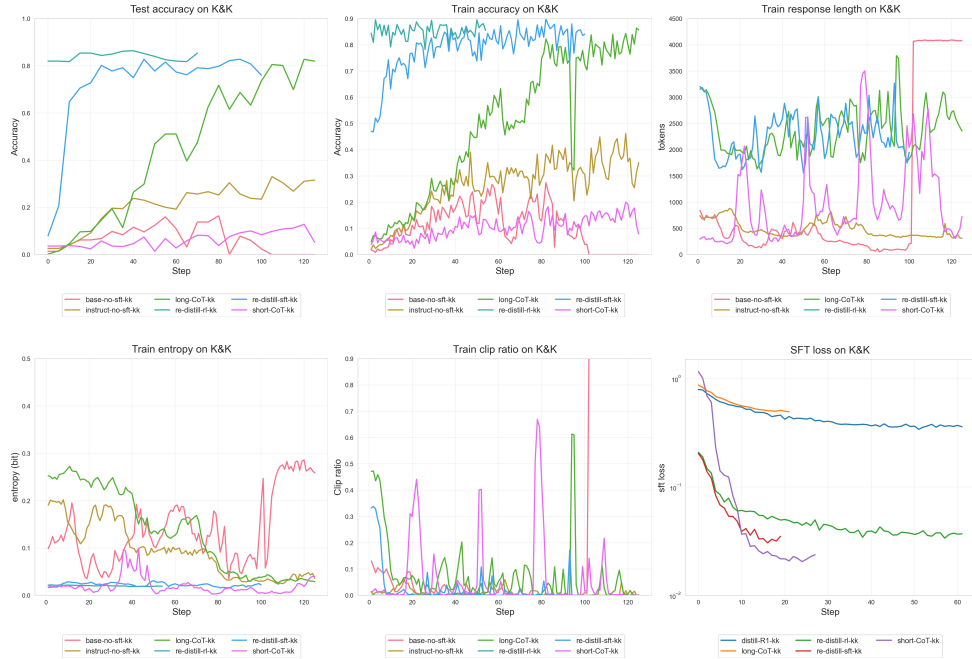


Fig. 9. Statistics in K&K dataset. **Top Left:** Test accuracy in RL. **Top Middle:** Train accuracy in RL. **Top Right:** Training response length(token) in RL. **Bottom Left:** Training entropy in RL. **Bottom Middle:** Training clip ratio(exceeding max response length in RL). **Bottom Right:** SFT loss curve.

G.3 Detailed Statistics on MATH dataset

We list detailed statistics for experiments on MATH dataset in Figure 10.

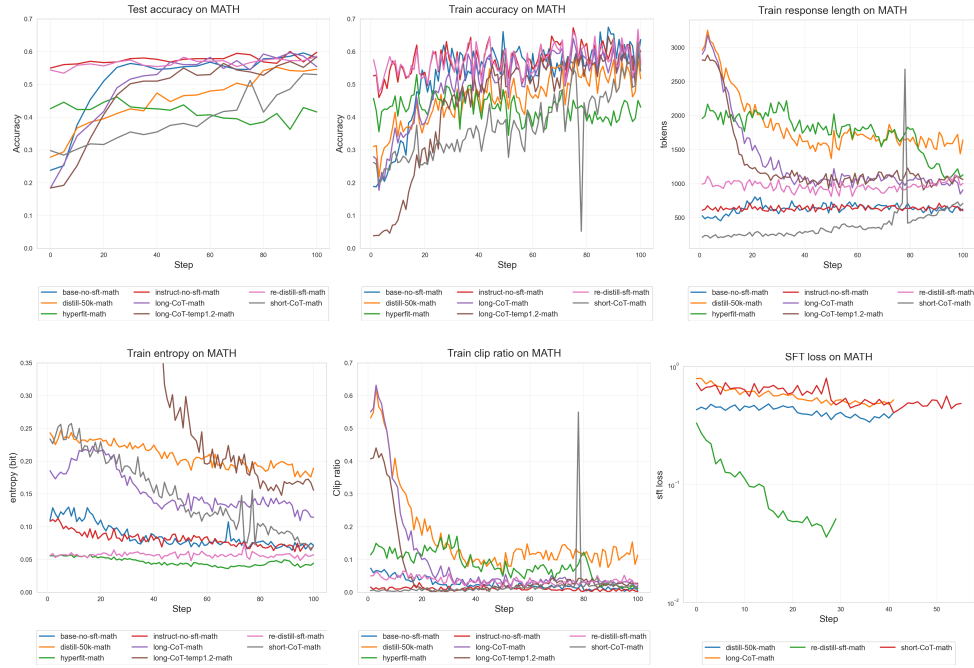


Fig. 10. Statistics in MATH dataset. **Top Left:** Test accuracy in RL. **Top Middle:** Train accuracy in RL. **Top Right:** Training response length(token) in RL. **Bottom Left:** Training entropy in RL. **Bottom Middle:** Training clip ratio(exceeding max response length in RL). **Bottom Right:** SFT loss in log scale.

H Prompt Templates

We use the following prompt templates for Qwen2.5-1.5B SFT, RL and evaluation. [QUESTION] can be MATH or K&K prompts.

Prompt templates for Qwen-2.5-1.5B SFT, RL and evaluation

```
<|im_start|>system\nPlease reason step by step, and put your final
answer within \\boxed{.}<|im_end|>\n<|im_start|>user\n[QUESTION]<|
im_end|>\n<|im_start|>assistant\n
```

We use the following prompt templates for DeepSeek-R1 Distilled Model's evaluation.

Prompt templates for DeepSeek-R1 Distilled Model

```
<|begin_of_sentence|><|User|>Please reason step by step, and put your
final answer within \\boxed{.} [QUESTION]<|Assistant|><think>\n
```

We use the following prompt templates for Qwen Base model.

Prompt templates for Qwen2.5-1.5B base model RL

```
Question:\n[QUESTION]\nAnswer:\nLet's think step by step.
```

I Output Mode classification

On K&K dataset, we classify output into 3 modes: `distill-no-wait` starts with ‘Okay’, an important signal in R1-style output, and contains ‘wait’ in lower or upper case. `distill-wait` starts with ‘Okay’ and does not contain any ‘wait’ word. If output does not start with ‘Okay’, we classify it into `others` mode.

On MATH dataset, we classify output into 3 modes: `long` starts with ‘Okay’ or ‘Alright’. `pretrain` starts with either of ‘To determine’, ‘To find’, ‘To compute’, ‘To solve’ or ‘To ensure’. They are top frequently appeared words in Qwen2.5-1.5B-Instruct output. Other outputs are clustered into `others` mode.

Our mode classification method is able to distinguish different modes. In Figure 11 left sub-figure, we sample from three models’ response on K&K test set. ‘Instruct’ denotes the Qwen2.5-1.5B Instruct; ‘RL-trained’ denotes the 125 steps checkpoint of long-CoT-kk; ‘Distilled’ denotes initial policy of long-CoT-kk. In right sub-figure, ‘Instruct’ denotes Qwen2.5-1.5B Instruct; ‘RL-trained’ denotes the 100 steps checkpoint of long-CoT-math and ‘Distilled’ denotes initial policy of long-CoT-math. There is a significant difference between instruct model output and R1-distilled output.

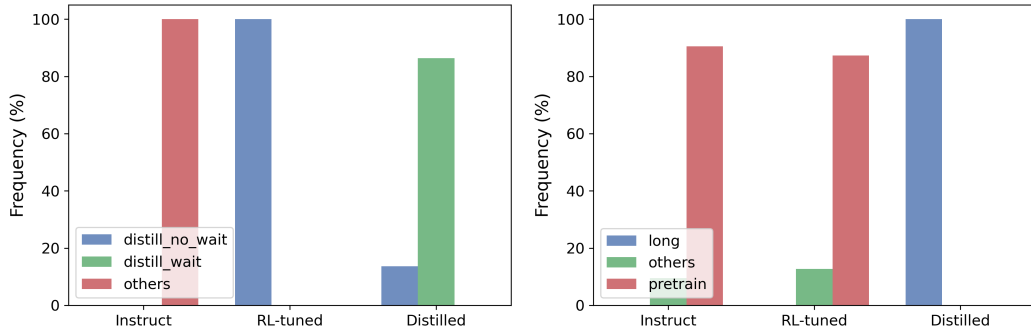


Fig. 11. **Left:** Mode proportions on K&K dataset. **Right:** Mode proportions on MATH dataset

J Qualitative study

Samples on K&K dataset are provided as follows:

Sample generated from long-CoT-kk, 125 step, 7 ppl correct answer

```

<|im_start|>system\nPlease reason step by step, and put your final answer within \\boxed{.}<|im_end|>\n<|im_start|>user\nA very special island is inhabited only by knights and knaves. Knights always tell the truth, and knaves always lie. You meet 7 inhabitants: Benjamin, Henry, Jack, Aurora, Jackson, Victoria, and Scarlett. According to Benjamin, \"Scarlett is not a knight\". Henry remarked, \"If Jackson is a knave then Victoria is a knight\". \"Victoria is not a knight,\" Jack mentioned. In Aurora's words: \"Jackson is a knight if and only if Jack is a knave\". Jackson asserted: \"Jack is a knave\". In Victoria's words: \"Jack is a knave or Henry is a knave\". Scarlett asserted: \"Aurora is a knave and Henry is a knave\". So who is a knight and who is a knave? Your final answer should be in this format: \\boxed{XX is a knave, YY is a knight, ...}<|im_end|>\n<|im_start|>assistant\nOkay, let's try to figure out who among Benjamin, Henry, Jack, Aurora, Jackson, Victoria, and Scarlett is a knight and who is a knave. Each of them is either a knight or a knave. Knights tell the truth and knaves lie. Each person makes a statement. Let's list their statements first:\n1. Benjamin says, \"Scarlett is not a knight.\"\\n2. Henry says, \"If Jackson is a knave then Victoria is a knight.\"\\n3. Jack says, \"Victoria is not a knight.\"\\n4. Aurora says, \"Jackson is a knight if and only if Jack is a knave.\"\\n5. Jackson says, \"Jack is a knave.\"\\n6. Victoria says, \"Jack is a knave or Henry is a knave.\"\\n7. Scarlett says, \"Aurora is a knave and Henry is a knave.\"\\n\nSince knights tell the truth and knaves lie. Let's consider Jackson's statement: \"Jack is a knave.\" Since Jack is a knight. Therefore, Jackson's statement is false. So Jackson is a knave.\nNow let's look at Aurora's statement: \"Jackson is a knight if and only if Jack is a knave.\" Since Jack is a knight. Therefore, the right side is false. The left side is \"Jackson is a knight.\" Since Jackson is a knave. Therefore, the right side is false. The left side is true. Therefore, Aurora's statement is false. So Aurora is a knave.\nVictoria's statement: \"Jack is a knave or Henry is a knave.\" Since Jack is a knight. Therefore, the

```

second part of Victoria's statement is false. Therefore, Victoria's statement is false. So Victoria is a knave.
Scarlett's statement: "Aurora is a knave and Henry

...

Since Aurora is a knight. Therefore, the first part of Scarlett's statement is false. Therefore, the second part of Scarlett's statement is "Henry is a knave." Since Henry is a knight. Therefore, the second part is false. Therefore, the entire statement is false. Therefore, Scarlett's statement is false. Therefore, Scarlett is a knave.
Benjamin's statement: "Scarlett is not a knight." Since Scarlett is a knave. Therefore, the statement is true. Therefore, Benjamin is a knight.
Victoria's statement: "Jack is a knave or Henry is a knave." Since Henry is a knight. Therefore, the second part of Victoria's statement is "Henry is a knave." Since Henry is a knight. Therefore, the second part is false. Therefore, the entire statement is "Jack is a knave." Since Jack is a knave. Therefore, the statement is true. Therefore, Victoria's statement is true. Therefore, Victoria is a knight.
All conditions are satisfied. Therefore, the final answer is:
, Jackson is a knight, Victoria is a knight, Scarlett is a knave}

Sample generated from long-CoT-kk, 0 step, 7 ppl wrong answer(response length exceeded)

<|im_start|>system\nPlease reason step by step, and put your final answer within \\boxed{.}<|im_end|>\n<|im_start|>user\nA very special island is inhabited only by knights and knaves. Knights always tell the truth, and knaves always lie. You meet 7 inhabitants: Benjamin, Henry, Jack, Aurora, Jackson, Victoria, and Scarlett. According to Benjamin, "Scarlett is not a knight". Henry remarked, "If Jackson is a knave then Victoria is a knight". "Victoria is not a knight", Jack mentioned. In Aurora's words: "Jackson is a knight if and only if Jack is a knave". Jackson asserted: "Jack is a knave". In Victoria's words: "Jack is a knave or Henry is a knave". Scarlett asserted: "Aurora is a knave and Henry is a knave". So who is a knight and who is a knave? Your final answer should be in this format: \\boxed{XX is a knave, YY is a knight, ...}<|im_end|>\n<|im_start|>assistant\nOkay, let's try to figure out who's a knight and who's a knave on this island. So we have seven people: Benjamin, Henry, Jack, Aurora, Jackson, Victoria, and Scarlett. Each of them made a statement. Let's break down each statement and see what we can deduce.\n\nFirst, let's list out the statements again for clarity:\n\n1. Benjamin: "Scarlett is not a knight".\n2. Henry: "If Jackson is a knave then Victoria is a knight".\n3. Jack: "Aurora is a knight if and only if Jack is a knave".\n4. Aurora: "Jackson is a knight if and only if Jack is a knave".\n5. Jackson: "Jack is a knave".\n6. Victoria: "Jack is a knave or Henry is a knave".\n7. Scarlett: "Aurora is a knave and Henry is a knave".\n\nHmm, that's a lot of statements. Let's start by considering the possibilities. Since knights always tell the truth and knaves always lie, we need to look for contradictions or consistent statements.\n\nLet's begin by assuming each person is a knight or a knave and see if that leads to a contradiction or a consistent solution.\n\nFirst, let's note that there are two possibilities for each person: they are either a knight or a knave. So there are $2^7 = 128$ possible combinations. But we need to narrow this down.\n\nLet's start by assuming Benjamin is a knight. If Benjamin is a knight, then his statement "Scarlett is not a knight" is true. Therefore, Scarlett is a knave. So if Benjamin is a knight, then Scarlett is a knave. Let's see if this leads to any contradictions.\n\nScarlett is a knave, then her statement "Jackson is a knight" must be a lie. Therefore, Jackson is a knave. So if Scarlett is a knave, then Jackson is a knave. Let's check if this holds with the other statements.\n\nHenry's statement: "If Jackson is a knave then Victoria is a knight". Since Jackson is a knave, the antecedent is true, so the implication is automatically true.\n\nTherefore, Henry's statement is true, so Henry is a knight. But wait, if Henry is a knight, then his statement is true, which is consistent. So far, so good.\n\nJack's statement: "Aurora is a knight if and only if Jack is a knave". Since Jack is a knight, the antecedent is true, so the implication is true. Therefore, Aurora is a knight. So if Jack is a knight, then Aurora is a knight. Let's check if this holds with the other statements.\n\nAurora's statement: "Jackson is a knave". Since Jackson is a knave and Jack is a knight, the statement is false. Therefore, Aurora is a knave. But wait, if Aurora is a knave, then her statement is false, which is consistent with Jackson being a knave. So far, so good.\n\nJackson's statement: "Jack is a knave". Since

...

Since Aurora is a knight and Henry is a knight, the statement is false. Therefore, Scarlett is a knave. But wait, if Scarlett is a knave, then her statement is false, which is consistent. So far, so good.\n\nWait, but let's check if there's another possibility. Let's assume Benjamin is a knave. If Benjamin is a knave, then his statement "Scarlett is not a knight" is a lie, so Scarlett is a knight. Let's see if this leads to a contradiction.\n\nIf Scarlett is a knight, then her statement "Jackson is a knight" is true. Therefore, Jackson is a knight. So if Scarlett is a knight, then Jackson is a knight. Let's check if this holds with the other statements.\n\nHenry's statement: "If Jackson is a knave then Victoria is a knight". Since Jackson is a knight, the implication is true. Therefore, Henry's statement is true, so Henry is a knight. But wait, if Henry is a knight, then his statement is true, which is consistent. So far, so good.\n\nJack's statement: "Aurora is a knight if and only if Jack is a knave". Since Jack is a knight, the antecedent is true, so the implication is true. Therefore, Aurora is a knight.

Sample generated from DeepSeek-R1, 2ppl, correct answer example

Okay, let's try to figure out who's a knight and who's a knave here. So, we have Harper and Elizabeth. Harper says, "Elizabeth is a knight and Elizabeth is a knave." Wait, that's a contradiction, right? Because someone can't be both a knight and a knave at the same time. So if Harper is a knight, then his statement must be true. But since the statement is a contradiction, that can't be possible. Therefore, Harper must be a knave. Because knaves always lie, so his statement is false. \n\nBut let's not jump to conclusions yet. Let's break it down step by step. Let's consider Harper first. If Harper is a knight, then both parts of his statement must be true. That would mean Elizabeth is a knight AND Elizabeth is a knave. But that's impossible because she can't be both. So Harper can't be a knight. Therefore, Harper must be a knave. So his statement is false. \n\nNow, Harper's statement is "Elizabeth is a knight and Elizabeth is a knave." Since Harper is a knave, the negation of his statement must be true. The negation of "A and B" is "not A or not B." So the negation would be "Elizabeth is not a knight OR Elizabeth is not a knave .\" But since everyone is either a knight or a knave, "Elizabeth is not a knight" is the same as "Elizabeth is a knave," and "Elizabeth is not a knave" is the same as "Elizabeth is a knight .\" So the negation simplifies to "Elizabeth is a knave OR Elizabeth is a knight." But since everyone is one or the other, this is always true. Hmm, so that doesn't give us new information. Wait, maybe I need to approach this differently.\n\nSince Harper's statement is a contradiction, regardless of whether he's a knight or knave, the statement itself is impossible. But since knights can't lie, if Harper were a knight, he couldn't make a false statement, but his statement is necessarily false. Therefore, Harper must be a knave. So that part is settled.\n\nNow, moving on to Elizabeth. She says, "Elizabeth is a knight or Harper is a knave." Let's analyze this. Let's consider two possibilities: Elizabeth is a knight or Elizabeth is a knave.\n\nFirst, suppose Elizabeth is a knight. Then her statement must be true. Her statement is "Elizabeth is a knight OR Harper is a knave." If she's a knight, then the first part of the OR is true, so the entire statement is true regardless of Harper's status. But we already determined Harper is a knave, so the second part is also true. So if Elizabeth is a knight, her statement holds. That seems consistent.\n\nAlternatively, suppose Elizabeth is a knave. Then her statement must be false. Her statement is "Elizabeth is a knight OR Harper is a knave." If she's a knave, then the first part is false. The second part, "Harper is a knave," we already concluded Harper is a knave, so that part is true. So the entire statement would be "False OR True," which is True. But since Elizabeth is a knave, her statement must be false. However, the statement evaluates to True, which contradicts her being a knave. Therefore, Elizabeth cannot be a knave. \n\nTherefore, Elizabeth must be a knight. \n\nWait, let me verify again. If Elizabeth is a knight, her statement is true. Her statement is "I am a knight OR Harper is a knave." Since Harper is indeed a knave, the OR statement is true. So that works. If Elizabeth were a knave, her statement would have to be false. But her statement is "I am a knight OR Harper is a knave." If she's a knave, then "I am a knight" is false, but "Harper is a knave" is true. So the OR of false and true is true. But since she's a knave, her statement must be false. But we just saw that it's true. Contradiction. Therefore, Elizabeth must be a knight. \n\nSo putting it all together: Harper is a knave because his statement is a contradiction, which can't be true. Elizabeth is a knight because her statement holds true and assuming she's a knave leads to a contradiction. \n\nTherefore, the conclusion is Harper is a knave and Elizabeth is a knight.\n\nFinally, write the answer in the boxed format: \\boxed{Harper is a knave, Elizabeth is a knight}.

Sample generated from K&K script, 2ppl, correct answer

Let's think step by step, by considering whether each person is lying and if that leads to contradiction. Assume Scarlett is a knight. No contradiction is found in their claim that If Jackson is a knight then Scarlett is a knight. Jackson cannot be a knight, because this would contradict the claim of their own that If Jackson is a knight then Scarlett is a knave. Jackson cannot be a knave, because this would contradict the false claim of their own that If Jackson is a knight then Scarlett is a knave. We have exhausted all possibilities for Jackson, so let us go back and reconsider Scarlett. Assume Scarlett is a knave. No contradiction is found in their false claim that If Jackson is a knight then Scarlett is a knight. Assume Jackson is a knight. No contradiction is found in their claim that If Jackson is a knight then Scarlett is a knave. This leads to a feasible solution.\n\nThe final answer is: \\boxed{Scarlett is a knave, Jackson is a knight}.

Samples on MATH dataset are provided as follows:

Short CoT for SFT, transformed to Qwen format, correct answer

```
<|im_start|>system\nPlease reason step by step, and put your final answer within \\boxed{.}<|\n|im_end|>\n<|im_start|>user\nJanaina is trying to solve the following equation by completing the\nsquare: $$x^2+18x-9 = 0. $$ She successfully rewrites the above equation in the following form: $$ (x\n+ b)^2 = c, $$ where $b$ and $c$ are integers. What is the value of $c$?<|im_end|>\n<|im_start|>\nassistant\nWe rewrite the equation as follows, trying to create a square of a binomial on the left
```

```
side: \begin{align*} nx^2 + 18x - 9 &= 0 \\ nx^2 + 18x + 81 &= 90 \\ (x + 9)^2 &= 90. \end{align*}
align*} We see that this clearly works, and $c = \boxed{90}.
```

DeepSeek-R1 generated long CoT for SFT, transformed to Qwen format, correct answer

```
<|im_start|>system\nPlease reason step by step, and put your final answer within \boxed{.}.<|im_end|>\n<|im_start|>user\nIf $a$ and $b$ are acute angles such that $\cos a = \frac{3}{5}$ and $\cos b = \frac{5}{13}$, then find $\cos(a + b)$.<|im_end|>\n<|im_start|>assistant\nOkay, so I need to find $\cos(a + b)$ where $a$ and $b$ are acute angles, and I know $\cos a = 3/5$ and $\cos b = 5/13$. Hmm, right. The formula for $\cos(a + b)$ is $\cos a \cos b - \sin a \sin b$. I remember that. So I have $\cos a$ and $\cos b$ already, which are $3/5$ and $5/13$. But I need $\sin a$ and $\sin b$ too. Since $a$ and $b$ are acute angles, their sines will be positive, right? Because in the first quadrant, all the trigonometric functions are positive. So I can use the Pythagorean identity $\sin^2 \theta + \cos^2 \theta = 1$ to find $\sin a$ and $\sin b$. Let me start with $\sin a$. If $\cos a = 3/5$, then $\sin a = \sqrt{1 - \cos^2 a} = \sqrt{1 - (9/25)} = \sqrt{16/25} = 4/5$. That seems straightforward. Similarly, for $\sin b$, since $\cos b = 5/13$, $\sin b = \sqrt{1 - (25/169)} = \sqrt{144/169} = 12/13$. Okay, so $\sin a$ is $4/5$ and $\sin b$ is $12/13$. Now plugging these into the formula: $\cos(a + b) = (3/5)(5/13) - (4/5)(12/13)$. Let me compute each part step by step. First, $(3/5)(5/13)$. The $5$ in the numerator and denominator cancels out, so that's $3/13$. Then the second term is $(4/5)(12/13)$. Let's multiply those: $4*12 = 48$ and $5*13 = 65$, so that's $48/65$. Now plugging these into the formula: $\cos(a + b) = 3/13 - 48/65$. To subtract these fractions, they need a common denominator. The denominators are $13$ and $65$. $65$ is a multiple of $13$ ($13*5=65$), so I can convert $3/13$ to $15/65$ (since $3*5=15$). Then subtract $48/65$ from that: $15/65 - 48/65 = (15 - 48)/65 = -33/65$. Wait, so $\cos(a + b)$ is $-33/65$? But $a$ and $b$ are acute angles, which means each is between $0$ and $90$ degrees. So $a + b$ would be between $0$ and $180$ degrees. Cosine is positive in the first quadrant ($0$ to $90$) and negative in the second quadrant ($90$ to $180$). So if $a + b$ is more than $90$ degrees, the cosine would be negative. Since both $a$ and $b$ are acute, their sum could be up to $180$, but given that each is less than $90$, the maximum sum would be less than $180$. Wait, actually, if both are acute, each is less than $90$, so the sum is less than $180$. But depending on their measures, the sum could be in the second quadrant. For example, if $a$ is $60$ and $b$ is $60$, the sum is $120$, which is in the second quadrant. So getting a negative cosine makes sense here. But let me check my calculations again to make sure I didn't make a mistake. Let's go through each step again. First, $\cos a = 3/5$. So $\sin a = \sqrt{1 - (3/5)^2} = \sqrt{1 - 9/25} = \sqrt{16/25} = 4/5$. Correct. $n \cos b = 5/13$. So $\sin b = \sqrt{1 - (5/13)^2} = \sqrt{1 - 25/169} = \sqrt{144/169} = 12/13$. Correct. $n \cos(a + b) = \cos a \cos b - \sin a \sin b = (3/5)(5/13) - (4/5)(12/13)$. The first term: $3/5 * 5/13$. The $5$ cancel, leaving $3/13$. The second term: $4/5 * 12/13$. Multiply numerators: $4*12=48$, denominators: $5*13=65$. So $48/65$. Then, $3/13$ is equivalent to $15/65$. So $15/65 - 48/65 = -33/65$. That seems right. $n \cos(a + b)$ is $-33/65$. Let me just confirm once more. Maybe I can check with decimal approximations. Let's compute $a$ and $b$ in degrees, maybe? $n \cos a = 3/5$. So $a = \arccos(3/5)$. Let me compute that. $3/5$ is $0.6$. $\arccos(0.6)$ is approximately $53.13$ degrees. Similarly, $\cos b = 5/13 \approx 0.3846$. $\arccos(0.3846)$ is approximately $67.38$ degrees. So $a + b \approx 53.13 + 67.38 \approx 120.51$ degrees. Then $\cos(120.51)$ degrees. Let's compute that. $120$ degrees is in the second quadrant, and $\cos(120$ degrees) is $-0.5$. Let's compute $\cos(120.51)$. Using calculator, $\cos(120.51) \approx \cos(180 - 59.49) = -\cos(59.49) \approx -0.5075$. Now, $-33/65$ is approximately $-0.5077$, which is very close. So that checks out. So the answer is indeed $-33/65$. $n \cos(a + b)$ is $-33/65$. Therefore, the final answer is \boxed{-\frac{33}{65}}.
```

Re-distilled sample from long-CoT-math step 50 checkpoint, wrong answer

```
<|im_start|>system\nPlease reason step by step, and put your final answer within \boxed{.}.<|im_end|>\n<|im_start|>user\nGiven positive integers $x$ and $y$ such that $\frac{1}{x} + \frac{1}{2y} = \frac{1}{7}$, what is the least possible value of $xy$?<|im_end|>\n<|im_start|>assistant\nOkay, let's solve the equation $\frac{1}{x} + \frac{1}{2y} = \frac{1}{7}$ for positive integers $x$ and $y$, and find the least possible value of $xy$. Let's start by expressing the equation in a more manageable form. First, combine the fractions on the left-hand side: $\frac{1}{x} + \frac{1}{2y} = \frac{2y + x}{2xy} = \frac{1}{7}$. So, we have: $\frac{2y + x}{2xy} = \frac{1}{7}$. Cross-multiplying gives: $7(2y + x) = 2xy$. Expanding and rearranging terms: $14y + 7x = 2xy$. Rearrange to form a quadratic equation in terms of $x$: $7x - 2xy + 14y = 0$. To solve this, we can add $14y$ to both sides: $7x - 2xy + 14y = 14y$. Factor out $x$ on the left-hand side: $x(7 - 2y) = 14y$. Thus, $x = \frac{14y}{7 - 2y}$. Since $x$ is a positive integer, $7 - 2y$ must also be an integer. Therefore, $7 - 2y$ must be a divisor of $14y$. Let's denote $7 - 2y = d$, where $d$ is a divisor of $14y$. Then, $x = \frac{14y}{d}$. This implies $2y = d + 7$, so $y = \frac{d+7}{2}$. Since $y$ is a positive integer, $d+7$ must be even, so $d$ must be odd. Also, $d$ must divide $14y$. Let's express $y$ in terms of $d$: $y = \frac{14y}{d} = \frac{14y}{d+7} \cdot \frac{d+7}{d+7} = \frac{14y}{d+7}$. For $x$ to be a positive integer, $\frac{14y}{d+7}$ must be an integer, so $d+7$ must be a divisor of $14$. The divisors of $14$ are $1, 2, 7, 14$. Since $d$ is odd, $d+7$ must be even, so $d$ can be $1, 3, 5, 7, 9, 11, 13$. Therefore, $d$ can be $1, 3, 5, 7, 9, 11, 13$. Now, let's check each case. If $d = 1$, then $x = 14y$ and $y = 7$, so $xy = 98$. If $d = 3$, then $x = 14y$ and $y = 11$, so $xy = 154$. If $d = 5$, then $x = 14y$ and $y = 13$, so $xy = 182$. If $d = 7$, then $x = 14y$ and $y = 9$, so $xy = 126$. If $d = 9$, then $x = 14y$ and $y = 7$, so $xy = 98$. If $d = 11$, then $x = 14y$ and $y = 5$, so $xy = 70$. If $d = 13$, then $x = 14y$ and $y = 3$, so $xy = 42$. Therefore, the least possible value of $xy$ is $42$.
```

$\frac{1+7}{2} = 4$, $x = 7 + \frac{49}{14} = 7 + 7 = 14$. If $d = 7$, $xy = 7 + 7 = 14$. If $d = 49$, $xy = 7 + 1 = 8$. Comparing the three values, the minimum value of xy is 84. Therefore, the least possible value of xy is $\boxed{84}$.

Qwen2.5-1.5B Instruct repsonse, correct answer

system
 Please reason step by step, and put your final answer within $\boxed{\text{.}}$.
 system
 user
 Ringo was roping a recalcitrant dogie. Ringo decided to give the dogie a reprieve by calculating $|(1-i)^8|$ before riding after the dogie. What answer should Ringo have found?
 system
 To find the value of $|(1-i)^8|$, we need to follow these steps:
 1. Express $(1-i)$ in polar form:
 The complex number $(1-i)$ can be written in polar form as $r e^{i\theta}$, where r is the magnitude and θ is the argument.
 2. Calculate the magnitude r :
 The magnitude r of a complex number $a+bi$ is given by $\sqrt{a^2+b^2}$. For $(1-i)$, $r = \sqrt{1^2+(-1)^2} = \sqrt{2}$.
 3. Determine the argument θ :
 The argument θ of a complex number $a+bi$ is given by $\tan^{-1}\left(\frac{b}{a}\right)$. For $(1-i)$, $\theta = \tan^{-1}(-1) = -\frac{\pi}{4}$.
 4. Write $(1-i)$ in polar form:
 Using the magnitude r and the argument θ :

$$(1-i) = \sqrt{2} e^{-i\frac{\pi}{4}}$$
.
 5. Raise $(1-i)$ to the 8th power:
 Using De Moivre's Theorem, which states that for a complex number $r e^{i\theta}$:

$$(r e^{i\theta})^n = r^n e^{in\theta}$$
. For $(1-i)^8$, $r = \sqrt{2}$ and $\theta = -\frac{\pi}{4}$.

$$(1-i)^8 = \left(\sqrt{2}\right)^8 e^{-i8\frac{\pi}{4}} = 16 e^{-2\pi i} = 16$$
.
 Therefore, the answer Ringo should have found is $\boxed{16}$.